UNIVERSITA' DEGLI STUDI
DI PADOVA
Dipartimento di Fisica e Astronomia
Dipartimento di Ingegneria Industriale

ISTITUTO NAZIONALE
DI FISICA NUCLEARE
Laboratori Nazionali di Legnaro

Under the Auspice of the TESLA TECHNOLOGY COLLABORATION

MASTER THESIS

in

"Surface Treatments for Industrial Applications"

RF Characterization of Thin Film Sputtered Superconducting Resonators

Supervisor: Prof. V. Palmieri
Co-Supervisor: Dott. C. Pira

Student: Giovanni Caldarola
N. Matr.: 1111606

Academic Year 2014-2015

Abstract

Long time has passed from the discovery of superconductivity, in 1911. Since then theoretical and experimental progress have been made continually. Nevertheless, there are still much to learn about superconductivity and the uses of superconducting materials. At INFN/LNL research and development is being done in order to understand the properties and uses of various superconducting materials to push forward the field of particle accelerator technology. These are used to fabricate radio-frequency (RF) accelerating cavities in order to minimize the power dissipated and increase their figures of merit, such as accelerating gradient (E_{acc}) and intrinsic quality factor (Q_0 or Q) which is a convenient parameter for the number of oscillations it takes the stored energy to dissipate to zero.

Superconducting properties of high purity niobium makes it the preferred material for many accelerator projects using superconducting technology. In fact, niobium possesses very intriguing physical and mechanical properties, not only the highest superconducting transition temperature (T_c) of 9.26°K and the highest superheating field of 240 mT among all available superconducting pure metals but also excellent ductility, which enables machining to be done relatively easily. In addition, the high quality factor and cavity accelerating gradient are fundamental parameters as they affect the overall cost of the accelerator in a direct way.

The accelerating gradient of the superconducting niobium cavities has been remarkably raised in the past decades with an advance of the cavity fabrication technology.

Cavities used to-date are made of niobium either in bulk or niobium coated on copper and are operated at 1.8 and 4.2 °K where the BCS component of the surface resistance is reduced to minimum and the cavity works in the residual resistivity regime.

In Legnaro three laboratories are reserved for cavity treatments and analysis: the chemical, the sputtering and the cryogenic lab, which is dedicated to the whole process of RF testing.

The work will focus on the influence on cavity performance of external surface conditions (in bulk cavity) and of the interface between niobium and copper (in thin film sputtered cavities). Specifically the interest is aimed to investigate how to better allow heat transfer from the resonator to the helium bath

For this purpose, 6 GHz elliptical cavities have been used. The main advantages over a 1.3 or 1.5 GHz superconducting RF cavities (SRF) are saving time, cost and material. Furthermore, due to smaller dimensions, the processes involved have been characterized by a reduction of energy in thermal treatments and a fast cryogenic measurement. A spinning technology is used to create seamless bulk-Nb and bulk-Cu cavities [1].

As a parallel activity, RF characterization of a 101 MHz Nb-Cu QWR (quarter wave resonator) has been conducted and compared with previous tests, varying sputtering parameters.

During the RF test the cavities have to be cooled at cryogenic temperatures in order to reach the superconducting state. In the testing facility there are two apertures which can host a cryostat and allow that this task is accomplished. While 6 GHz elliptical cavities are tested at 4.2°K and then at 1.8°K, for the 101 MHz QWR a temperature of 4.2°K is sufficient.

Contents

Chapter 3

Chapter 4

Chapter 1

A brief introduction to Superconductivity and SC cavities

1.1 *An overview*

Superconductivity is the ability of certain materials to conduct electric current with practically zero resistance. This produces interesting and potentially useful effects. For a material to behave as a superconductor, low temperatures are required. Superconductivity was first observed in 1911 by H. K. Onnes, a Dutch physicist who succeeded in liquefying helium in 1908 [2]. His experiment was conducted with elemental mercury at 4.2°K, the temperature of liquid helium. He observed that the electrical resistance disappeared completely near the T_c temperature (fig. 1.1), characteristic for each material. He said, "*Thus, mercury at 4.2°K has entered a new state which owing to its particular electrical properties can be called the state of superconductivity*".

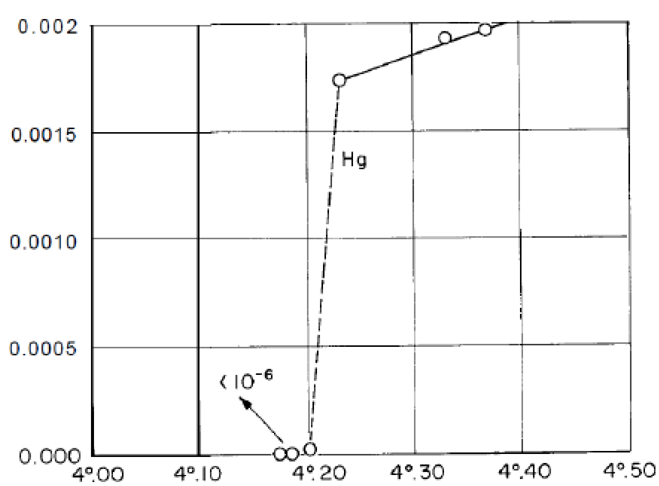

Figure 1.1. *The original plot by H. Kamerlingh Onnes shows absence of resistance below 4.2°K.*

There is also an intimate relation between superconductivity and magnetic fields.

In 1933 W. Meissner and R. Ochsenfeld performed an experiment that triggered development of theories of superconductivity [3]. They discovered that a superconducting element like lead expels a weak magnetic field from its interior when cooled below T_c, while in stronger fields superconductivity breaks down and the material goes to the normal state. The spontaneous exclusion of magnetic fields upon crossing T_c cannot be explained in terms of the Maxwell equations of classical electrodynamics and indeed turned out to be of quantum-theoretical origin. Shortly after C.J. Gorter and H. Casimir suggested that upon superconducting transition a number of electrons turn ”super” and these, now ”super” electrons, can carry a big current without losses. As the temperature goes closer to absolute zero the number of ”super” electrons increases and the number of normal electrons decreases.

A large number of elements and compounds (mainly alloys and ceramics) have been found showing superconductive behavior. For superconducting cavities, niobium shows the most interesting properties.

1.2 *Superconductor surface resistance*

For a direct current or low frequency alternating currents the superconducting electrons shield the normalconducting electrons from the electromagnetic field so that no power is dissipated. On the contrary, alternating currents at microwave frequencies behave differently. The inertia of the Cooper pairs prohibits them to follow the changing electromagnetic fields immediately, the shielding is not perfect. The normalconducting electrons start to flow and dissipate power. This gives rise to a resistance which depends on the number of normalconducting electrons and the frequency of the alternating current. For temperatures $T < T_c/2$ and energy of the microwave photons of $hf << \Delta$ the surface resistance can be approximated by:

$$R_{BCS}(T,f) = A\frac{f^2}{T}e^{\left(\frac{-\Delta}{k_B T}\right)} \quad (1)$$

The factor A depends on material parameters like coherence length, electron mean free path, Fermi velocity and penetration depth. For niobium the factor A is about $9\text{x}10^{-5}$ ΩK/(GHz)^2.

1.3 *Residual resistance*

The total surface resistance also contains a temperature independent part, which is called residual resistance R_0. The residual resistance is usually dominated by lattice imperfections, chemical impurities, adsorbed gases and trapped magnetic field. Well prepared niobium surfaces show a residual resistance of a few nΩ [4].

$$R_S = R_{BCS}(T) + R_0 \tag{2}$$

Much is reported in literature about the possible origin of the residual resistance: both “physical phenomena” and “accidental mechanisms” (like dust, chemical residuals or surface defects on the cavity walls) contribute to parasitic losses. Due to the variety of the phenomena involved, it is very hard to express a formula that can predict them.

1.4 *Superconducting cavities*

A superconducting cavity is the device used to provide energy to the particles that are crucial to an accelerator. Radio frequency (RF) cavities have been in use for nearly five decades to accelerate the ion beam to ever increasing higher energies in a particle accelerator. Exploration of RF superconductivity for particle accelerators begun in 1965 with the acceleration of electrons in a lead plated cavity [5]. There are two main categories of particle accelerating structure, which depends on the velocity (v) of the particle to be accelerated. Usually, a parameter β that is defined as v/c where c is the velocity of light is used to separate the two types. When $0.5< \beta<1$, this is typical for accelerating electrons with kinetic energy of a few MeV and protons with 100 MeV. Figure 1.2 shows a typical Nb Superconducting RF cavity for this group of particle accelerating structures where a chain of five coupled RF cells are resonating in the transverse magnet mode.

In this field configuration, the longitudinal electric field is maximized along the axis of the cavity and the RF phase between adjacent cells is 180° as schematically illustrated in the upper part of figure 1.2. In this way, a particle with velocity close to the speed of light will experience the maximum acceleration in each cell of the cavity [6].

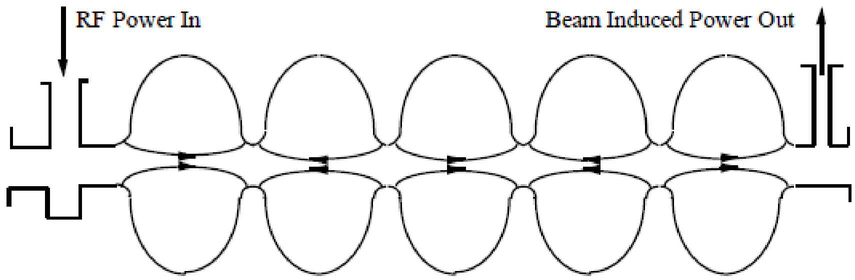

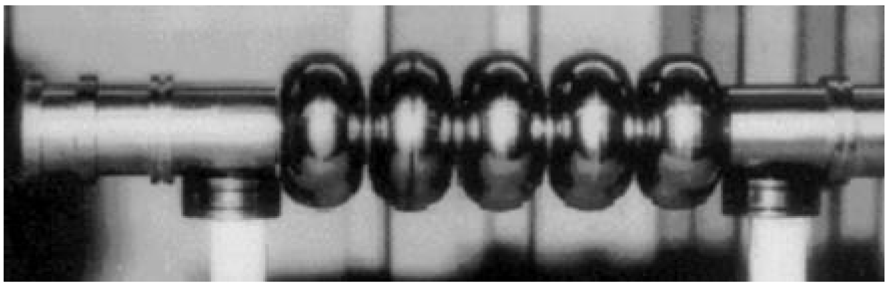

Figure 1.2. *The typical Nb SRF accelerating structure consists of a chain of cavities and its side view. The cavity is fabricated from bulk Nb, and cooled in a bath of liquid He at temperature 4.2°K (Courtesy of* ACCEL)

It is essential to operate Nb cavities at below 2°K to obtain high accelerating gradient combined with high Q factor. Liquid helium below 2°K is a superfluid with extremely high thermal conductivity and is, thus, an excellent coolant. Nb cavities are accordingly operated at between 1.5 and 1.8°K. Generally, the performance of a SCRF cavity is characterized by an excitation curve where the quality factor Q is plotted as a function of the accelerating gradient E_{acc}.

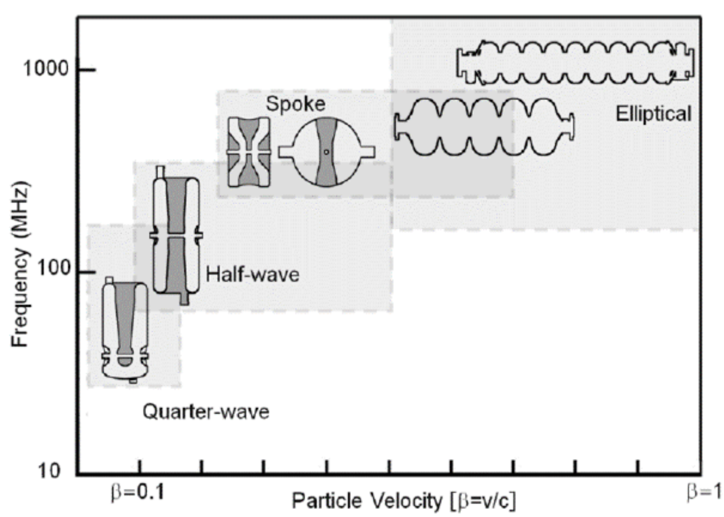

Figure 1.3. Classification of accelerating structures. [7]

A $\beta < 0.5$, that is for "slow" particle, is typical for accelerating ions from helium to uranium with kinetic energies from a few to 20 MeV per nucleon. For this group, a variety of different accelerating structures may exist [6] as schematically depicted in figure 1.3. ALPI linac at Laboratori Nazionali di Legnaro (LNL) works with quarter wave resonator (QWR) (figure 1.4).

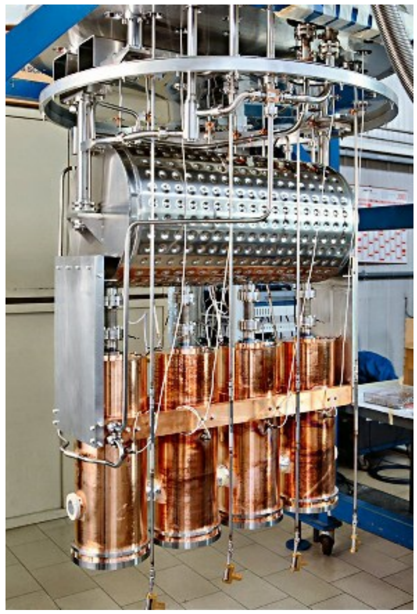

Figure 1.4. Four accelerating high purity copper-based cavities at ALPI linac (LNL). Cavity inner surface is coated by a niobium thin layer.

1.5 *Advantages of superconductive cavities*

Although not completely loss free above T = 0°K, as in the dc case, superconducting cavities dissipate orders of magnitude less power than normal conducting accelerating structures. The dramatically reduced resistivity translates into a number of very important advantages. They include:

1. *Operating cost savings*: Even when taking into account the cost of refrigerating superconducting cavities, their power demand in continuous wave (CW) applications is less than that of equivalent copper cavities.
2. *Capital cost savings*: The reduced power requirements translate into capital cost savings, since fewer (and sometimes simpler) klystrons are needed.

3. *High gradient*: The relatively low power consumption also enables superconducting cavities to operate at high CW gradients.
4. *Reduced impedance*: The aperture of superconducting cavities is large; thereby minimizing disruptive interactions of the cavity with the beam, higher currents can therefore be accelerated.

1.6 *6 GHz cavity fabrication technique*

In order to improve the characteristics of the cavity at LNL the spinning fabrication technique is used. This technology has several advantages in comparison with welding:

- short fabrication time;
- equipment could be adapted for any size of the cavity, and any quantity of cells;
- comparably low fabrication costs;
- no intermediate annealing;
- almost no scraps;

The process of spinning of the 1.5 GHz cavity is depicted on figure 1.5. However, it is also used for producing 6 GHz Nb cavities.

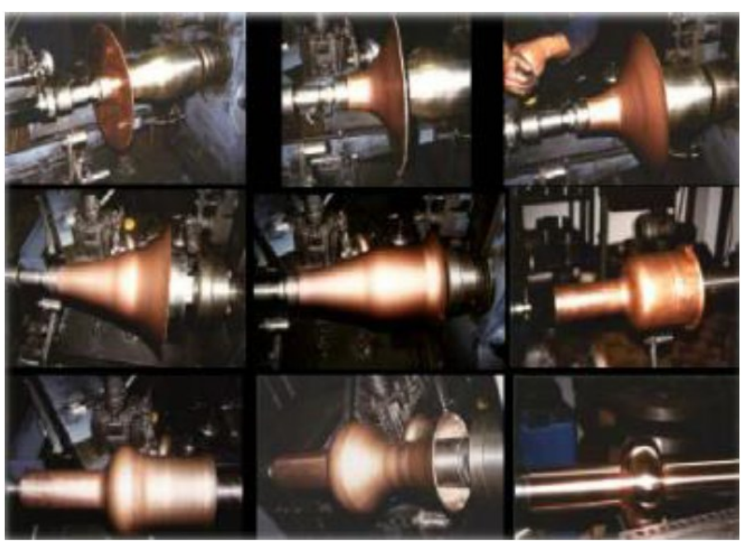

Figure 1.5. *Various steps during the fabrication of a 1.5 GHz copper monocell cavity by spinning.*

The process is mainly divided in three steps. A circular disk of 400 mm diameter and 3 mm thickness is first preformed onto a frustum shaped mandrel, the first half-cell is formed and a cylindrical shape is given to the remaining part of the piece, by means of a second pre-mandrel. The second step consists in spinning the obtained artifact onto a collapsible mandrel that has exactly the same shape of the cavity interior, up to when the roller overcomes the equator and fixes the piece to spin onto the mandrel. Then, the third and last step consists in inserting a further frustum-shaped collapsible mandrel in order to guide the material when spinning the second half-cell. Both collapsible mandrels are then removed.

1.7 *6 GHz Cavity geometry*

6 GHz cavities are 97 mm long and have a 45 mm diameter cell (fig. 1.6 and fig. 1.7). They are made through the spinning technology using larger cavities fabrication remaining material.

Due to the spinning process, the mechanical stress of the material is considerable and the imprints caused by the internal collapsible mandrel must be removed. The cleaning procedure is similar to the one used for bigger cavities: mechanical treatments, chemical treatments and electro-polishing are sequentially performed to try to improve the surface quality [8].

These type of cavities are extremely light and easy to handle: they can be quickly mounted on a suitable stand and they can be measured directly by immersion in a liquid helium bath.

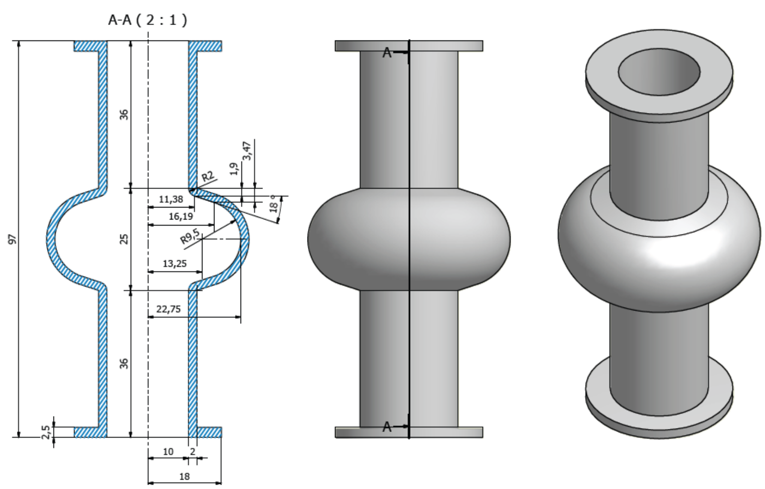

Figure 1.6. *A schematic diagram of 6 GHz tesla type Nb mono cell SRF cavity.*

Figure 1.7. *A Nb 6 GHz cavity.*

1.8 *101 MHz QWR*

The Quarter Wave resonator (fig. 1.8) is a basic resonant structure that consists of a length of transmission line shorted at one end and "open" at the other end, the length is nearly a quarter of the free space wavelength of the lowest resonator frequency. The high impedance at the opened extremities can be used to accelerate the particles, building up high voltages needed for particle acceleration. The QWR was created in 1981 for heavy ion acceleration [9].

The main advantages of the QWR are the following:

- a broad curve of the transit time factor,
- a structure which is simple to manufacture and electrically balanced,
- high frequency of the lowest mechanical mode,
- low peak surface field values,
- efficient cooling of the inner conductor,
- elimination of the end plates which are necessary in split loop and spiral resonators and which can be a source of frequency drifts and lossy joints.

Mostly, QWRs are used in the acceleration of low velocity ions. These types of cavities can been made using different materials (lead-plated copper, niobium explosively bonded to copper, pure niobium metal and niobium sputtered on cooper). For full details see [7].

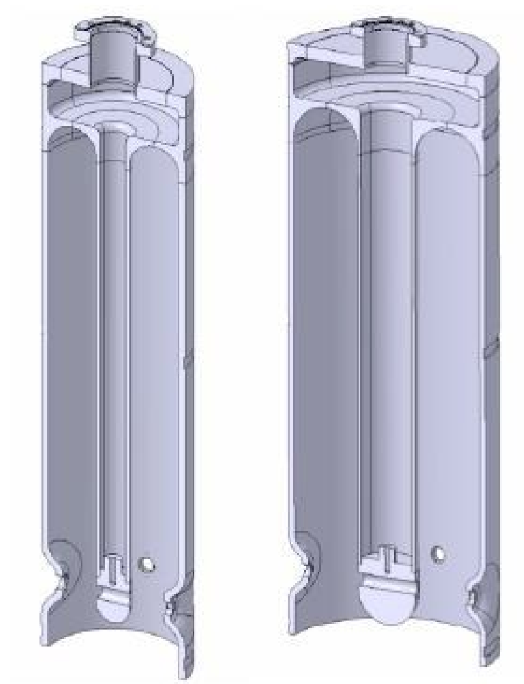

Figure 1.8. High-β (left) and low-β (right) *101 MHz QWR cavity design.[7]*

1.9 *Properties of Niobium*

Niobium is a chemical element having symbol Nb and atomic number 41. It is a transition metal which belongs to group V in fifth period of the periodic table. It is a ductile transition metal, soft, gray in appearance. It was initially named columbium. Now the mineral is also called "niobite", which is well used not only for scientific research but also for commercial purpose, such as: in special steel alloys, welding, electronics, optics, nuclear industries, and jewelries.

Among all existing superconducting elements, it has the highest critical SC transition temperature. The research group led by W. Meissner reported the discovery of superconductivity in niobium at T_c=9.2°K [10] in 1930. Niobium is the pure element with the highest T_c under normal conditions. The critical temperature measured in monocrystal high purity niobium (RRR=5000) was reported to be 9.2877°K [11].

Atomic number	41
Atomic weight	92,9 g/mol
Atomic radius	2.08
Density	8570 kg m^{-3}
Crystalline lattice	b.c.c.
Space group	Im3m
a	3,3033
Electrical resistivity (300K)	14.9 $\mu\Omega\cdot$cm
Thermal conductivity (300K)	53.7 W $m^{-1}K^{-1}$
Debye Temperature	275K
Melting Point	2741K
Critical temperature	9.26K
Density	8570 kg m-3
Density	8570 kg m-3

Table 1.9. *List of the niobium properties.*

Chapter 2

Superconducting radiofrequency cavities

2.1 *Accelerating cavities*

Accelerating cavities are used to increase the energy of a charged particle beam. Hence, the cavity is a structure that most efficiently stores the electromagnetic energy when excited at the resonant frequency at one of its resonant modes. At resonance, the energy of the electric and magnetic fields is equal and is exchanged between the two ways at resonant frequency, and configuration of electric and magnetic field is defined and the field values periodically oscillate with time at the same frequency. Due to the low surface resistance, SC cavities can convert the RF input power in stored energy much more efficiently than the normal conducting cavities. Nevertheless, some other factors can limit their sustainable fields or their efficiency to transfer the electromagnetic energy to the beam. Obviously, the energy gain per unit length is therefore an important parameter of such devices. The accelerating voltage V_{acc} to which a particle with charge e is subjected while traversing the cavity is by definition:

$$V_{acc} = \left|\frac{1}{e} \times energy\ gain\ during\ transit\right| \tag{3}$$

For particles travelling at the speed of light *c* on the symmetry axis the accelerating voltage is given by:

$$V_{acc} = \left|\int_0^d E_z(z)\, e^{\frac{i\omega_0 z}{c}} dz\right| \tag{4}$$

where *d* is the length of the cavity and ω_0 is the eigenfrequency of the cavity mode under consideration.

The accelerating field is

$$Eacc = \frac{Vacc}{d} \tag{5}$$

Two other key parameters to characterize the superconducting accelerating structures are E_{pk} and H_{pk}, which denote the highest electric and magnetic field inside the resonant structure. Above this level the material becomes normal conducting ("quenches").

2.2 *RF – fields in cavities*

The RF fields in cavities are derived from the eigenvalue equation

$$\left(\nabla^2 - \frac{1}{c^2}\frac{\partial^2}{\partial t^2}\right)\left(\frac{E}{H}\right) = 0 \tag{6}$$

which is obtained by combining Maxwell's equations [12]. It is subject to the boundary conditions

$$\hat{n} \times \boldsymbol{E} = 0 \tag{7}$$

and

$$\hat{n} \times \boldsymbol{H} = 0 \tag{8}$$

at the cavity walls. Here:

- $\hat{n}$ is the unit normal to the RF surface;
- c is the speed of light;
- ***E*** and ***H*** are the electric and magnetic field, respectively.

In cylindrically symmetric cavities, such as the elliptical shape, the discrete mode spectrum given by equation 6 splits into two groups, transverse magnetic (TM) modes and transverse electric (TE) modes. For TM modes the magnetic field is transverse to the cavity symmetry axis whereas the electric field is transverse for TE modes. For accelerating cavities, therefore, only TM modes are useful.
The typical shape of speed of light cavities [13] is shown in figure 2.1.

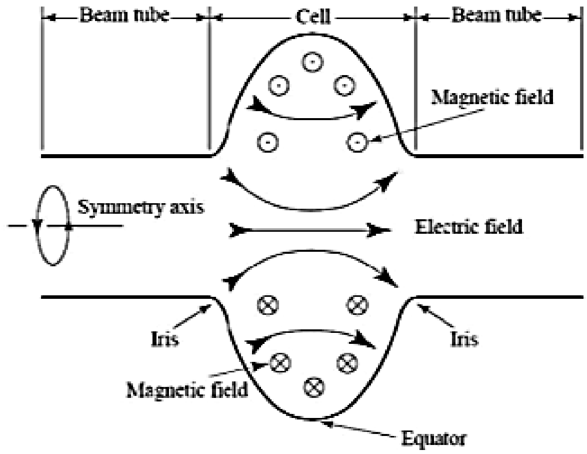

Figure 2.1. *Schematic of a generic speed-of-light cavity.*
The electric field is strongest near the symmetric axis, while the magnetic field is concentrated in the equator region

2.3 *Peak surface fields*

When considering the practical limitations of superconducting cavities, two fields are of particular importance: the peak electric surface field (E_{pk}) and the peak magnetic surface field (H_{pk}). These fields determine the maximum achievable accelerating gradient in cavities. The surface electric field is at its maximum near the irises, while the surface magnetic field is at its maximum near the equator. To maximize the potential cavity performance, it is important that the ratios of E_{pk} / E_{acc} and H_{pk} / E_{acc} are minimized.

2.4 *RF power dissipation and cavity quality*

In order to sustain the radiofrequency fields in the cavity, an alternating current is flowing in the cavity walls. This current dissipates power in the wall as it experiences a surface resistance. The power dissipated in the cavity, P_d, can be considered to define the global surface resistance R_{Surf} :

$$P_d = \frac{1}{2} \oint_A \; R_{Surf}\, H^2{}_{Surf} dA = R_{Surf} \oint_A \; H^2{}_{Surf}\, dA \qquad (9)$$

Here H_{Surf} denotes the magnetic field amplitude. Usually, the quality factor Q_0 is measured:

$$Q_0 = \frac{\omega_0 U}{P_d} \tag{10}$$

where

$$U = \frac{1}{2}\mu_0 \oint_V H^2\, dV \tag{11}$$

is the energy stored in the electromagnetic field in the cavity. R_{Surf} is an integral surface resistance for the cavity. The surface resistance and the quality factor are related via the geometrical constant G which depends only on the geometry of a cavity and field distribution of the excited mode, not on the resistivity of the material:

$$G = \frac{\omega\mu_0 \oint_V H^2 dV}{\oint_A H^2 dA} \tag{12}$$

This gives:

$$Q_0 = \frac{\omega_0\mu_0 \oint_V H^2 dV}{R_{Surf} \oint_A H^2 dA} = \frac{G}{R_{Surf}} \tag{13}$$

The quality factor can also be defined as

$$Q_0 = \frac{\omega_0}{\Delta\omega_0}$$

where ω_0 is the resonance frequency and $\Delta\omega_0$ the full width at half height of the resonance curve in an unloaded cavity. For the 6 GHz cavities used in our laboratory G = 287Ω. For a mono-cell elliptical niobium cavity the quality factor is typically > 10^{10} at T = 2°K. The efficiency with which a particle beam can be accelerated in a radiofrequency cavity depends on the surface resistance. The smaller the resistance, that is the lower the power dissipated in the cavity walls, the higher the radiofrequency power available for the particle beam. This is the fundamental advantage of superconducting cavities as their surface resistance is much lower and outweighs the power needed to cool the cavities to liquid helium temperatures.

2.5 *The Residual Resistivity Ratio (RRR)*

The Residual Resistivity Ratio (RRR) is a parameter that can be used to quantify the general impurity content of a material. For a relatively impure Nb, the dc resistivity ($\rho \approx 1/\sigma$) drops by a factor of 30 from its room temperature value of $15\text{x}10^{-8}$ Ωm in the normal state, to its residual value. The factor by which resistivity drops to the residual value is called the residual resistance ratio, RRR. The higher the RRR, the lower the impurity content of the material. It is important to point out here that there are background contributions to RRR value from phonons and grain boundaries. The RRR is defined as the ratio of the electrical resistivity at two temperatures: 300°K and 4.2°K.

The value of RRR indicates the low temperature thermal conductivity of a material as well, and is often used as a material specification for superconductors. For pure Nb used in RF cavities of linear accelerators, the low temperature resistivity is defined as the normal-state value extrapolated to 4.2°K, but this value does not differ much from the 10°K value.

$$RRR = \frac{\rho(300\ K)}{\rho_{extrap}(4.2\ K)} \tag{14}$$

In a sputtered cavity, the grain size and the purity of the thin film are such that the mean free path is very small (10-100 nm). Nevertheless, the Q_0 of such a cavity is twice that of a cavity made from high RRR bulk niobium.

RRR values serve as a convenient measure of the purity of the metal. High-purity niobium has higher RRR values. Calculated theoretical limit for RRR for Nb is 35000 and is determined by scattering of electrons by lattice vibration [14]. In practice, the highest RRR ever achieved for Nb is 33000 [15]. Generally speaking, a good Nb cavity should have E_{acc}>35 MV/m and Q_o>10^{10}. This would imply that the surface resistance should be less than a few tens of nΩ.

2.6 *Bulk niobium versus Nb thin film sputtered cavities*

While a perfect resonant cavity can be made by extensive efforts in the laboratory, there will be defects in real manufacturing, especially microscopic defects. The defects, which will heat up the local area by high surface current induced by the electromagnetic field, are one of the main issues in achieving high performance.

Since the thermal conductivity of the resonant cavity limits the amount of heat that can be dissipated to the cooling agent, to efficiently cool the resonant cavities the wall thickness could be reduced, while maintaining sufficient mechanical strength, improve the thermal conductivity of the cavity material, use thin film technology, or a different material with higher T_c and higher critical magnetic fields.

Since copper has a typical heat conductance, higher than the bulk niobium one, it is very easy for the copper substrate cavity to conduct the excessive heat to the helium bath. The large thermal conductivity of copper helps the thin film cavity to be more resilient.

Another important advantage in using Nb thin film on copper is that copper is much cheaper than niobium, about 1/10 the cost of the niobium. The material itself is not the only cost advantage: it is widely believed that the manufacturing cost associated with copper can be substantially lower than that of niobium.

A problem that Nb thin film cavities experience is that the Q-factor drops significantly with increasing accelerating fields, and thus inhibits the use of Nb thin film cavities []. There is strong evidence that film properties such as micro structure, grain size and granularity influences the rf performance. Another issue under investigation is the thermal boundary resistance at the interface between thin film and substrate.

2.7 *Thermal boundary resistance*

When there is a heat flow Q from a hot solid into liquid helium, the temperature of the solid surface remains higher than that of the helium bath by an amount

$$\Delta T = R_K Q \tag{15}$$

where R_K is the thermal boundary resistance, or Kapitza resistance, at the liquid-solid interface. It is a measure of an interface resistance to thermal flow. Due to the differences in electronic and vibrational properties in different materials, when an energy carrier (phonon in the present work) attempts to traverse the interface, it will scatter at the interface. The manifestation of a thermal boundary resistance has evolved as an intriguing phenomenon of considerable attraction for researchers since 1941, when Kapitza first observed the onset of a temperature jump on the boundary between superfluid helium and copper when a heat flux is passed through the boundary itself [16]. This subject is extremely complex and not completely understood.

Understanding the thermal resistance at the interface between two materials, in our case Nb-Cu, is of primary significance in the study of its thermal properties and this is technologically important for the optimization of superconducting RF cavity performances, where heat dissipation is strongly necessary.

A widely used predictive model was the acoustic mismatch model proposed by Khalatnikov [17], which assumes a geometrically perfect interface and an entirely elastic phonon transport across it, treating phonons as sound waves. Accordingly, the transfer of acoustic energy across the interface would be governed by acoustic principles; however, the predicted values for R_K were far too high compared to the experimental results.

Following a recent study [18] to be published by the end of 2015, a sputtered Nb-Cu thin film cavity can be described as a set of three subsystems:

- the superconducting niobium film;
- the copper substrate;
- the niobium–copper interface;

of which the last is investigated in our tests.

The hypothesis in reference [18] focuses on the Nb film adhesion over Cu substrate, considering therefore the problem of poor thermal contact between film and substrate as the main factor determining the high Q-slope observed in Nb thin film coated Cu cavities compared to bulk Nb cavities (fig. 2.2).

In their opinion, for several reasons, in most cases the Nb film is not strongly bonded over the full cavity surface and this results on the presence of limited cavity surface portions in which the high boundary resistance could fully dominate the heat conduction. Accordingly, these poor thermal contact areas will be gradually driven into the normal state, giving rise to a progressive micro-quench process.

Figure 2.3 shows the hypothetical temperature distribution along the normal direction to the cavity surface.

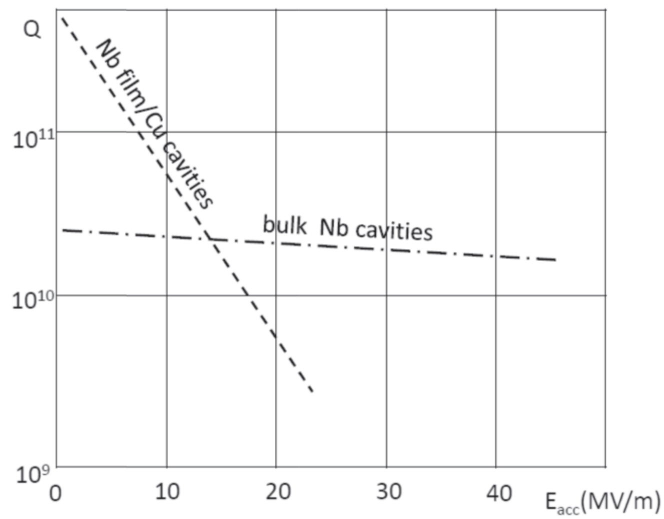

Figure 2.2. *Q-factor versus the accelerating field for bulk niobium cavities compared to Nb film sputtered cavities. Typical behavior is schematically reported for 1.3–1.5 GHz cavities at low temperatures (1.7–1.8°K).*

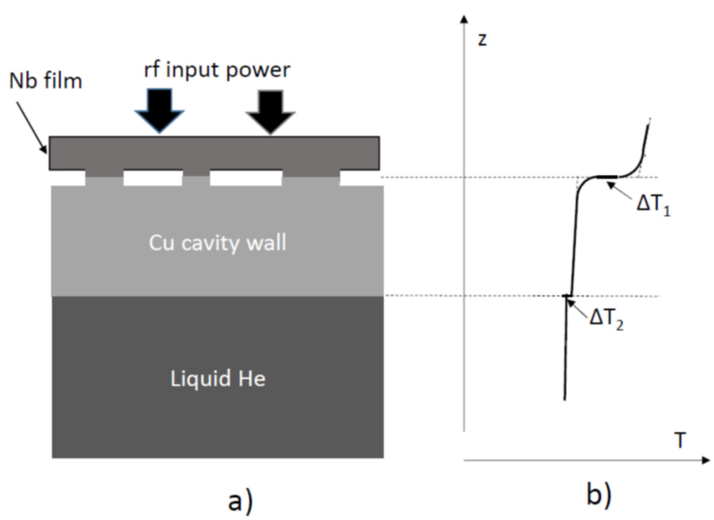

Figure 2.3. *Schematic view of the adopted one-dimensional thermal model (a) and the related temperature profile (b).*

Chapter 3

RF test system

3.1 *Fundamental equations for RF test*

During the RF tests on cold cavities the basic RF properties such as maximum accelerating gradient, field emission onset, and quality factor Q, as a function of gradient are determined. These tests are done inside the cryostat where the cavity is held vertically. In addition, to improve the systematic errors, setting the fundamental power coupler at or near critical coupling reduces the RF power requirement to a value close to that required for cavity wall losses.

The critical variable for calculating the RF parameters of a superconducting cavity is the shunt impedance, which relates the stored energy to the effective accelerating gradient. That is, along with cavity geometry, the necessary parameter for calculating peak electric field, and peak magnetic field for any given mode.

When a cavity mode oscillates with a resonant frequency ω_0, a stored energy U and RF losses on the cavity walls, P_d, the quality factor can be defined as:

$$Q_0 = \frac{\omega_0 U}{P_d} \tag{16}$$

Q_0 is 2π times the ratio of the stored energy and the energy consumed in one period. In the frequency domain the Q_0 can also be expressed as

$$Q_0 = \frac{\omega_0}{\Delta\omega_0} \tag{17}$$

where $\Delta\omega_0$ is the 3-dB band width. Unfortunately, the direct measurement of the 3-dB band width of a superconducting cavity is practically impossible, because it can attain very small values as compared to the center frequency: some Hz or fractions of Hz out of thousands of Megahertz. This is much less than the resolution of any commercially available network or spectrum analyzer. For this reason, a time domain method must be used.

The cavity receives the RF power via an input cable and an input antenna (coupler) from a power amplifier driven by a signal generator which is locked, as explained in the following chapters, exactly onto the resonant frequency of the cavity mode.

The transmitted power is extracted from the cavity by the output antenna (pickup probe).

All antennas are connected to calibrated power meters and it is possible to calculate the total power lost P_L with the following power balance:

$$P_L = P_d + P_{cpl} + P_{pk} \tag{18}$$

where P_d is the power dissipated in the cavity walls, P_{cpl} is the power leaking back out the fundamental power coupler and P_{pk} is the power transmitted out via pickup antenna.

This equation is valid for a cavity with no driving term that has a stored energy U.

In this condition the so called "*Q loaded*" is introduced to take into account the resonant circuit behavior when it is coupled with an external line:

$$Q_L = \frac{\omega_0 U}{P_L} \tag{19}$$

The quality factor, for each dissipated power, could be written as:

$$Q_0 = \frac{\omega_0 U}{P_d} \qquad Q_{cpl} = \frac{\omega_0 U}{P_{cpl}} \qquad Q_{pk} = \frac{\omega_0 U}{P_{pk}} \tag{20}$$

Those Q values are proportional to the number of cycles the system needs to dissipate all the energy on the considered transmission line. It is important to control if the dissipated power in the couplers is higher or lower that the power dissipated on the cavity walls.

It follows that:

$$\frac{1}{Q_L} = \frac{1}{Q_0} + \frac{1}{Q_{cpl}} + \frac{1}{Q_{pk}} \tag{21}$$

Each transmission line has its own external coupling factor β defined by:

$$\beta_x = \frac{Q_0}{Q_x} = \frac{P_x}{P_d} \quad (x = cpl, pk) \tag{22}$$

The transmission antenna should be sized in order to avoid perturbation of the cavity operation; this condition is reached when $\beta_{pk} << 1$; in this way the antenna picks up the bare minimum energy requested for the measurement. Moreover, its position, respect to the coupler antenna, is far enough to avoid the signal transmission without resonance inside the cavity (no cross-talking). On the other side, to be able to transfer all the input power to the cavity, the coupler should satisfy the condition $\beta_{cpl}= 1$ (critical coupling). These conditions assure a perfect match of the system and the cavity electrical impedances (coupling). In fact when $\beta_{cpl}= 1$ the input power equals the power dissipated in the cavity plus the small amount of power that goes out of the pickup port:

$$P_d = P_i - P_{ref} \tag{23}$$

where P_i is the incident power, P_{ref} is the reflected power and one assumes that $P_{pk} << P_d$.
Impedance matching is essential, otherwise a mismatch causes power to be reflected back to the source from the boundary between the high impedance and the low impedance. The reflection creates a standing wave, which leads to further power waste. The impedance matching device is the antenna tuner. In cases where β is not equal to 1, such as systems with a fixed input antenna or cavities when used to accelerate beam, the termination of the stored energy becomes more complex. Details on the calculation necessary for such cases are given in reference [19]. Fortunately, our system allows us to achieve critical coupling prior to doing a decay measurement. This simplifies the math and allows us to make several assumption which are described below.
When switching off the power supply, the cavity enters into a state of free decay, loosing energy due to dissipation on the cavity walls and the power flowing through the input and the output antennas. During a free decay, the power lost corresponds to the variation with time of the stored energy, thus:

$$\frac{dU}{dt} = -P_L = -\frac{\omega_0 U}{Q_L} = -P_d - P_{pk} - P_{cpl} \tag{24}$$

the solution (assuming that Q_L is independent of U) is an exponential decay, with

$$U = U(0)e^{-\frac{t}{\tau}} \qquad \tau = \frac{Q_L}{\omega_0} \tag{25}$$

The decay time constant τ is experimentally measured and it is used to calculate a value for the loaded-Q, Q_L. Then Q_L, P_i, P_{ref} , P_{pk} are used to calculate Q_0. In fact, when the cavity is critically coupled:

$$Q_0 = \left(1 + \beta_{cpl} + \beta_{pk}\right)Q_L = 2Q_L = 2\omega_0\tau \tag{26}$$

$$Q_{pk} = \frac{2\omega_0\tau\left(P_i - P_{ref} - P_{pk}\right)}{P_{pk}} \tag{27}$$

In summary, measuring P_i, P_{ref} , P_{pk} and τ are sufficient to derive Q_0 and Q_{pk}. The next step is increasing the incident power P_i in order to raise the stored energy value U. Q_{pk} is a constant that is strictly dependent on the probe/cavity geometry. Thus, using Q_{pk} the Q_0 and E values can be calculated from the measured values of

$$Q_0 = \frac{Q_{pk}P_{pk}}{P_i - P_{ref} - P_{pk}} \tag{28}$$

The gradient may then be calculated as:

$$E = \sqrt{Q_{pk}P_{pk}\frac{r/Q}{L^2}} \tag{29}$$

3.2 *RF system*

The Q measurement and RF processing of superconducting resonator can take advantage of computer controlled processes, which control the devices, collect data and assist the operator during the measurements. A block diagram of the measurement apparatus is shown in figure 3.1 and figure 3.2 for both the TESLA type and QWR cavities.

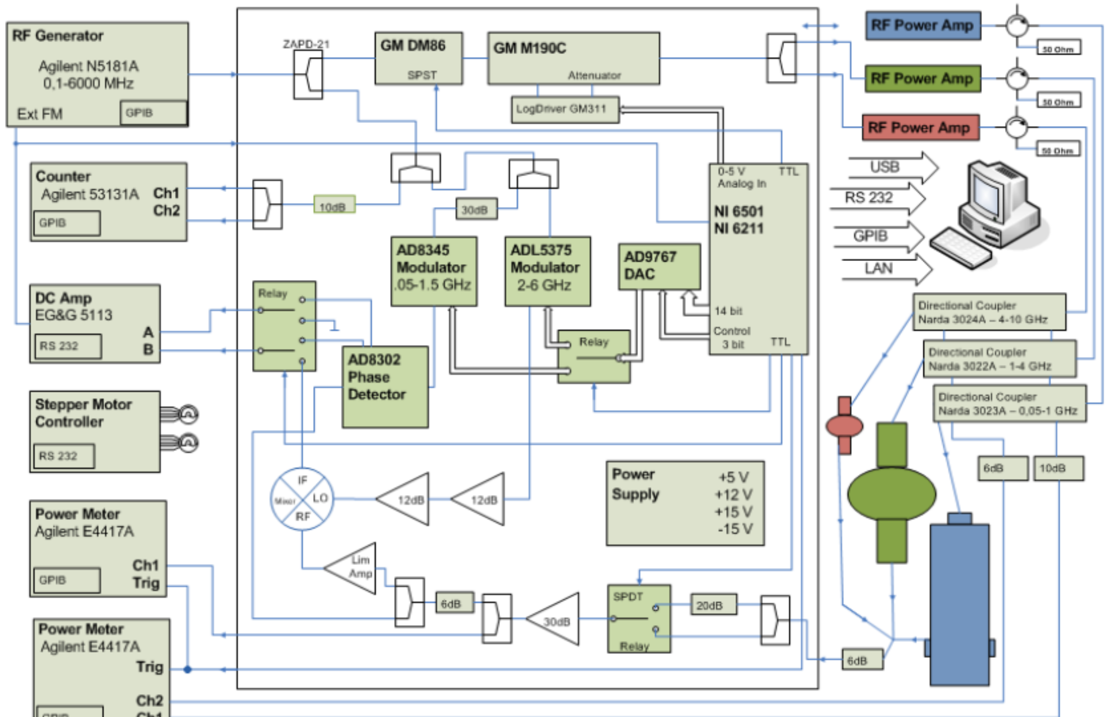

Figure 3.1. *A schematic of the RF test apparatus for* 6 GHz cavity (TESLA type)

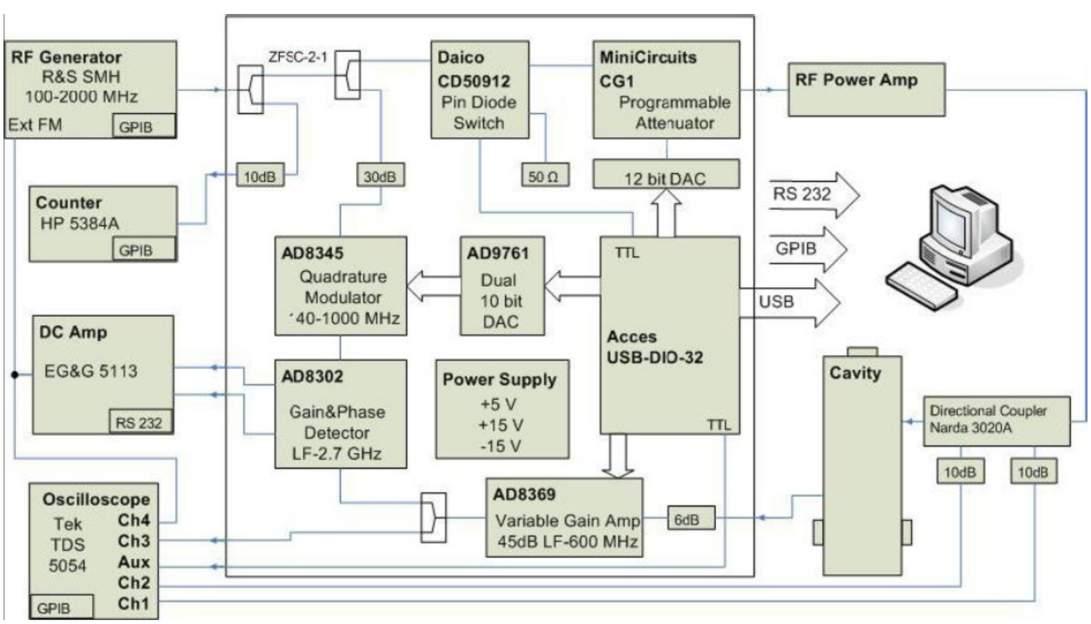

Figure 3.2. *A schematic of the RF test apparatus for* 101 MHz cavity (QWR)

The computer is interfaced with the signal generator, the power meter, the peak power analyzer and the frequency counter via IEEE 488 bus. These components are communicated with a unique chassis that includes all the other low power RF components. Analog devices components perform the functions of the phase shifter, phase detector and variable gain amplifier. The operating frequency determines the choice of the power amplifier. A dedicated computer board allows the acquisition of analog and digital inputs and the setting of digital and analog outputs. Figure 3.3 shows the measurement system for cavity testing.

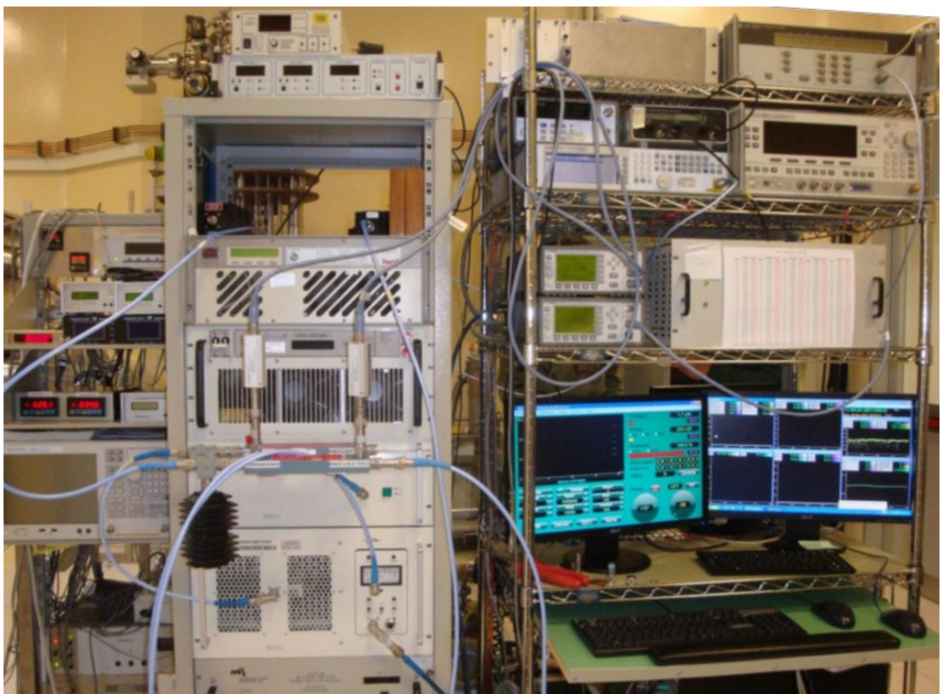

Figure 3.3. SRF 6 GHz cavity measurement system. This figure shows an image of the racks that consists of a set of instruments required to test an SRF cavity. This includes RF power heads, RF amplifier, RF generator, Frequency counter, dual directional coupler, RF box, oscilloscopes, DC amplifier, user interface and measuring computer.

The RF generator signal is divided into three paths. One goes through the programmable phase shifter to feed the mixer's local oscillator input. Once the cavity frequency is determined, the loop phase is adjusted such that the pickup signal (i.e. stored energy) is maximized. A second line goes to the frequency counter. The third is routed to the power amplifier (choice of which depends on the cavity frequency), via a PIN diode switch and a variable attenuator. The output of the amplifier is used to drive the fundamental coupler of the cavity. Depending on the coupling factors Q_L and Q_0, the cavity reacts as mismatch in the circuit and reflects back to the amplifier part of the incident power. The bi-directional coupler allows one to monitor the forward and reflected powers immediately at the input to the cavity since some of the power at input is reflected back. If no directional coupler was used, an interference between the forward and reflected powers could occur. Some of the power is reflected back at the input coupler while most of the power is transmitted through the cavity to be detected on the other side by the pickup antenna. Each of the three powers: forward, reflected and transmitted, are then split enabling a scalar measurement to be made using a power meter.

The first operation is finding the value of ω_0 using the computer program developed for the task (see section 3.5). The RF signal frequency (ω) that feeds the cavity, is produced by the RF generator. Since it can be different from the cavity resonant frequency (ω_0), it is necessary to set up a feedback loop in order to correct the frequency and to follow its variations in time. These variations are mainly due to microphonics, Lorentz force detuning, temperature and pressure changes: all of them modify the cavity geometry (and thus the frequency) by minor amounts. The operator looks at the input-output phase difference $\Delta\phi$ versus frequency, which is swept by the generator. The signal proportional to $\Delta\phi$ is used as a feedback to correct the delivered frequency. When the phase shift is properly adjusted the system will track variations in the cavity frequency.

The mixer output is a dc signal proportional to the phase difference between P_{pk} and P_i. The limiting amplifier (cavity output line) and the phase shifter (cavity input line) correct the initial value and keep low the difference of phase. Thus, the working point of the sweep generator is controlled by the output of the mixer to close the loop. Finally, the frequency is measured with a Frequency Counter. A DC amplifier with programmable gain closes the frequency loop [19].

Since the Q value of the cavity is calculated by means of an RF balance of power, forward, reflected and transmitted power levels at the cavity ports must be precisely measured. To this aim it is important to properly measure and compensate for all of the intervening circuit elements. In the system this cable calibration process is semi-automated and the calculations are done using the computer.
Input and output ports (on the top plate of the cryostat) are connected to the cavity antennas through two cables: they are referred to as *internal* because they have to be closed into the cryostat with the cavity. Obviously, it is important to measure both the external and internal cables dissipations, before starting the RF test.

As mentioned above, during the cavity RF test two antennas have to be attached to the resonator to drive the signals in and out: the *coupler*, which is the forward RF power antenna feeding the cavity, and the *pickup*, which allows collecting a small signal proportional to the electromagnetic field level inside the cavity (consequentially to the square root of the cavity stored energy). In this way we can follow the resonator energy change.

The coupler antenna position inside the cavity is adjustable (linear feedthrough plus bellow). Changing the coupler location we can modify the coupling conditions and consequently the transferred power and the resonator Q_L (and the related bandwidth).

We can distinguish three different cases: if the resonator is seen as a perfect matched load by the source, the coupling is critical, if the cavity impedance exceeds the feeding line one we speak about under-coupling, if the cavity impedance is lower than the feeding line one we have an over-coupling.

In critical coupling conditions, if we start feeding the cavity with constant power at its resonant frequency, the energy in the resonator rises until it reaches an equilibrium value at which time all the power transferred to the cavity is used to balance the losses. During the decay procedure, RF power is switched off and the cavity stored energy starts decreasing until it vanishes.

In a critical coupling condition, Q_{cpl} has to be approximately equal to the cavity quality factor ($Q_{cpl} \approx Q_{cavity}$).

The pickup antenna should collect a signal sufficient to drive the RF control loop. However, the power transmitted by the pickup should be a small fraction of the power dissipated in the superconducting resonator so to reduce the measurement errors. A Q_{pk} between 10 and 100 times higher than the cavity Q is a good compromise.

3.3 *Cryogenic apparatus*

During the test, the cavity has to be cooled at cryogenic temperatures in order to reach the superconductive state. The transition temperature for Nb is 9.26°K. The systems are typically operated at very low temperatures in order to better simulate actual accelerator operating conditions.

In the RF testing facility at LNL there are two apertures which can host a cryostat. One of them is used to test, simultaneously, three single cell 6 GHz elliptical type cavities; the other is used for

QWRs or single cell elliptical type cavities larger than the 6 GHz. Both cryostats have been designed and realized directly at LNL.

6 GHz elliptical type cavity infrastructure

This cryostat has been designed for operating at 4.2°K and 1.8°K and can contain up to three single cell cavity stands. Figure 3.4 shows the structure design along with a schematic picture.

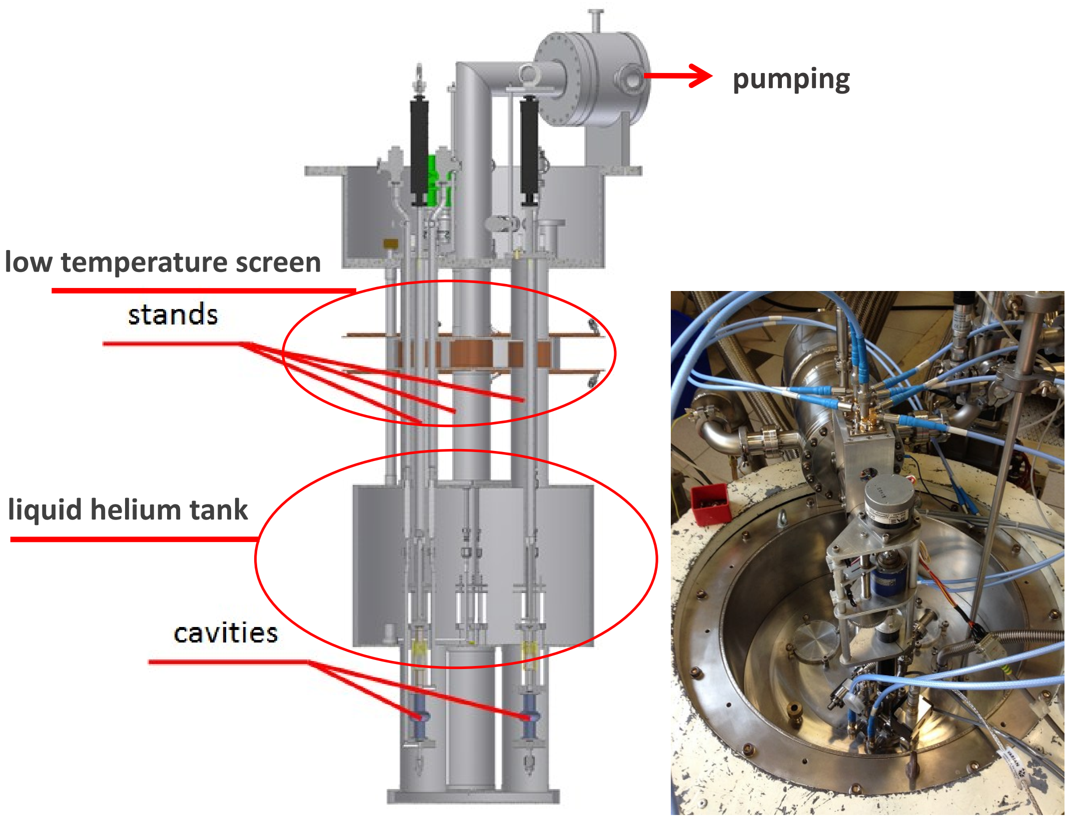

Figure 3.4. *6 GHz cavity cryostat design (left) and site picture (right).*

The infrastructure is composed by two liquid cryogen vessels containing respectively liquid helium and liquid nitrogen interspersed by two vacuum chambers, the outer being under vacuum to thermally insulate the sides. At the top, thermal insulation is improved by several copper screens.

A preliminary cooling is achieved by injecting liquid nitrogen in the second cryogen vessel. When the nitrogen level, measured by a dedicated probe, reaches its maximum, the liquid helium vessel is filled up to the temperature of 4.2°K. The transfer does not stop until the liquid level reaches the top of the helium tank. The cavity is then tested at 4.2°K.

To test the cavity at 1.8°K, it is necessary to reduce the gas pressure by further pumping over the helium bath.

QWR infrastructure

Even this cryostat has been designed for operating at 4.2°K and 1.8°K. It can be used to test both TESLA type (1.5 GHz) and, thanks to a later adaptation designed by D.A. Franco Lepinasse [7], QWR (Quarter Wave Resonator) cavities (fig. 3.5).

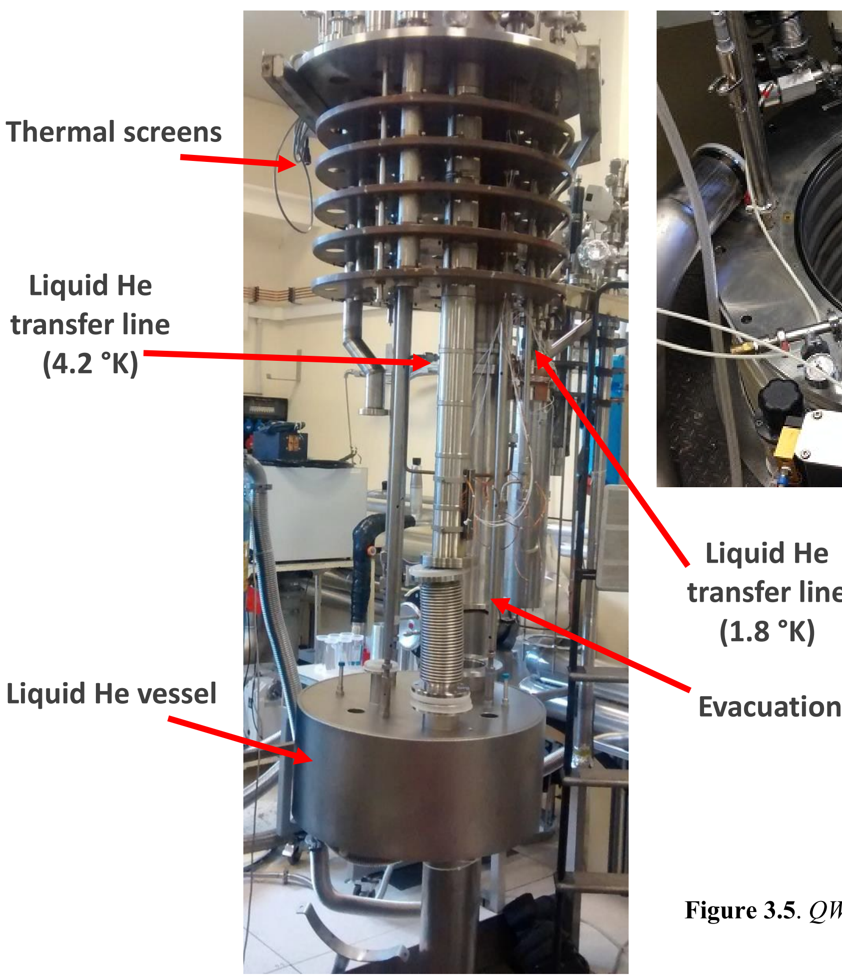

Figure 3.5. *QWR (101 MHz) cavity cryostat (left) and bunker picture (right).*

The infrastructure, obviously larger than the previously mentioned, in the same way, is composed by two liquid cryogen vessels, one for liquid helium and one for liquid nitrogen, interspersed by two vacuum chambers. It must be remarked that in tests performed with QWR cavities, the resonators are cooled from the inside (fig. 3.6). At the top, thermal insulation is improved by several copper screens cooled with the recovery helium cold gas.

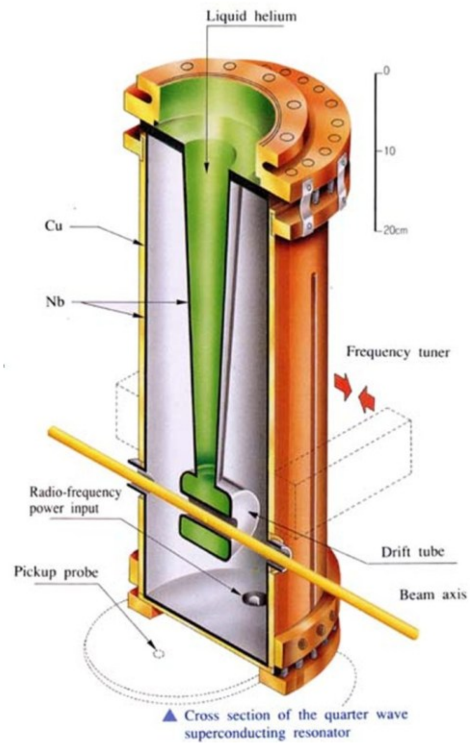

Figure 3.6. Cutaway view of a superconducting QWR resonant cavity. Liquid helium is injected from the top. (picture from http://rrsys.tokai-sc.jaea.go.jp/rrsys/html/tandem/english/koumoku-03/booster.html)

The cooling starts using the liquid nitrogen of the second chamber while the helium vessel is maintained at atmospheric pressure, and a thermal contact is created between the helium vessel and the liquid nitrogen vessel by filling the chamber in the middle with helium gas at 200mBar (exchange gas). Once the temperature reaches 100°K, the helium gas is removed from the intermediate vessel and the transfer of liquid helium at 4.2°K into the cavity starts. The cavity is tested at 4.2°K.

The above mentioned systems are both equipped, at their top flanges, with a set of RF and thermal feedthroughs as well as safety valves and other valves to connect the pumping system. The pumping systems includes different combination of pumps which work at different speed ranges: rotary and scroll pumps to reach a vacuum of $10^{-2}/10^{-3}$ mbar and turbomolecular pump to reach a base vacuum of $10^{-6}/10^{-7}$ mbar.

Since the purpose of a cryogenic system is to generate and maintain very low temperatures, a suitable network of temperature sensors is needed. The temperature monitoring system in the cryostat is undertaken by three kinds of sensors: diode thermometers, carbon glass resistor and germanium resistance thermometers.

The cavities are mounted on the vacuum system before starting the pumping procedure.

3.4 *Preparation and measurements procedure of 6 GHz cavity*

The vertical stand in use to perform the 6 GHz cavities RF tests is shown in figure 3.6.

To oversimplify the system assembling, the bottom part of it has been rendered completely independent (figure 3.7); in this way the small cavity can be mounted without the presence of the complete stand that would make the work complicated. Cavities are assembled inside class 1000 clean room.

Two stainless steel flanges close the cavity extremities using kapton O-ring and grease: one side of the cavity faces the forward antenna while the other looks at the pickup antenna. At this point the assembled is screwed on a bellow flange (fig. 3.6 a) and thus connected to the pumping line of the vertical stand (fig. 3.6 c). The 5 mm diameter pumping tube is divided into three parts: one of them is welded to the cavity bottom flange, one, fixed to the top of the insert, is connected to an external valve and goes to the pumping system; the last section consists in a small bellow equipped with a VCR connection on both sides, added to easily connect the other two pieces.

On the insert top plate there is a linear feedthrough that, together with the bellow connected on the upper cavity flange, permits the coupler antenna motion. The RF cables are clearly visible too: they are embedded into two supports, thought to avoid their stresses or motions during the cavity measurement.

A couple of thermometers are screwed on the bottom flange of the bellow.

Four Teflon coated vertical bar lines preserve the system alignment and prevent blockage problems due to the freeze-over of the bellow upper flange during the liquid helium insertion step.

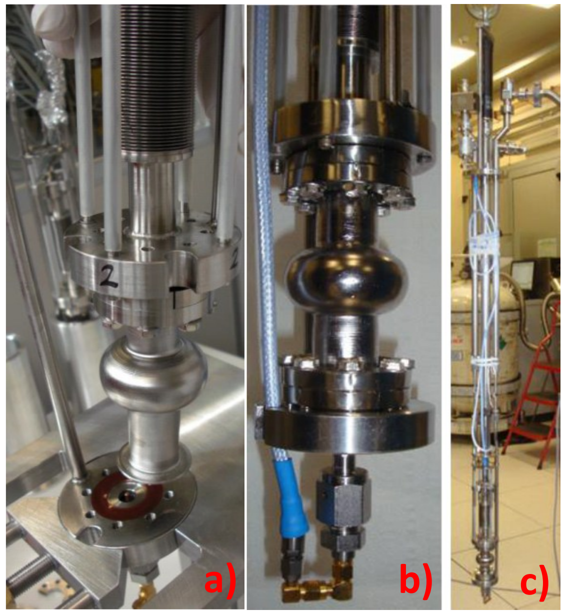

Figure 3.6. ***a)*** *Cavity mounting procedure on RF stand inside clean-room.* ***b)*** *Cavity screwed on forward power flange (top), and pick up flange (bottom).* ***c)*** *Cavity pumping lines are connected to RF stand.*

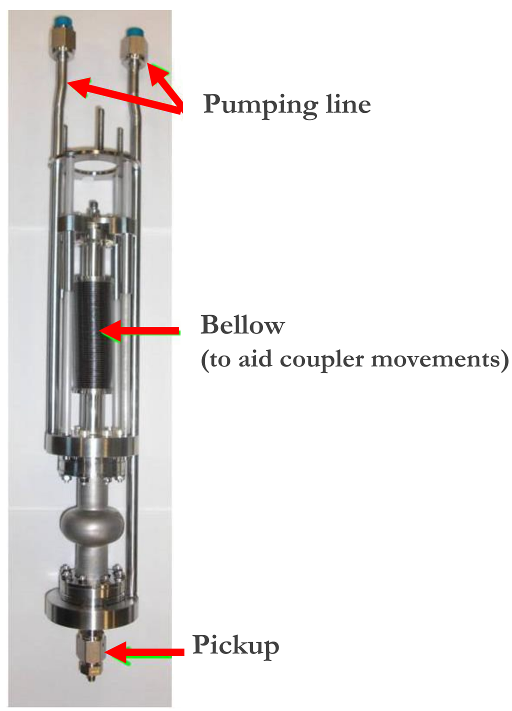

Figure 3.7. *An independent RF insert*

Next step is the pumping of the system to reach a pressure of approximately 10^{-7}-10^{-8} mbar prior to cooling at liquid helium temperature. This is achieved by means of a rotary, a turbo, and an ion-getter pumps. Most importantly, a great care must be taken to ensure that the vacuum system is thoroughly clean and dust free. The cavity itself is evacuated slowly to avoid turbulent flow and reduce risk of contaminants from the vacuum system reaching the cavity. For the same reason it is essential to maintain dust free condition while attaching input and output connectors to the cavity.

Pumping down to the final pressure usually takes several hours. After the ultimate pressure is reached, the RF stand is ready to be inserted inside the cryostat.

Meanwhile, the procedure of cooling the cryostat starts with the transfer of liquid nitrogen, first, then, while still injecting liquid nitrogen, the transfer of liquid helium begins and goes on until 4.2°K are reached. The lowest limit of 1.8°K is achieved by further pumping over the helium bath.

Once the superconductive state of the material is reached, the cavity is ready for the RF test. Two main parameters are measured, namely the Q_0 or quality factor of the equivalent resonant circuit vs. the electric field E_{acc}. These parameters are determined from a measurement of the decay time τ, incident, reflected and transmitted power (respectively P_i, P_{ref} and P_{pk}) and the resonant frequency of the cavity ω_0.

In order to search the cavity resonant frequency, the input-output phase difference as a function of frequency is observed. This value, which is used as a feedback signal to correct the frequency delivered by the generator, shows a visible variation around the resonant frequency.

Searching of the resonant frequency is done at low power (< 1W). Using such a low power it is possible to work local without any radiation risk.

In the superconductive state, the cavity band will be of a few Hertz so usually it is advisable to search the resonance at room temperature and then to lock the cavity before it gets superconducting, so that it is easier to find the center frequency in the cold state. After each sweep, the above mentioned phase difference is displayed on the computer as a function of frequency. The resonant frequency corresponds to a sharp variation which looks like a discontinuity (fig. 3.8).

Sometimes it could be easier to search for the frequency connecting the forward line to a Network Analyzer, which shows a negative peak in correspondence of the resonance (fig. 3.9).

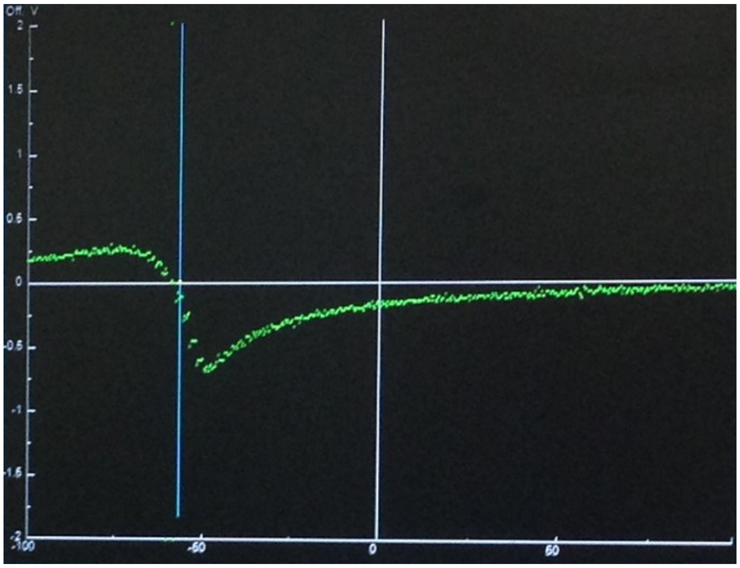

Figure 3.8. *Input-output phase difference versus frequencies.*
The sharp variation appears in correspondence to the resonant frequency.

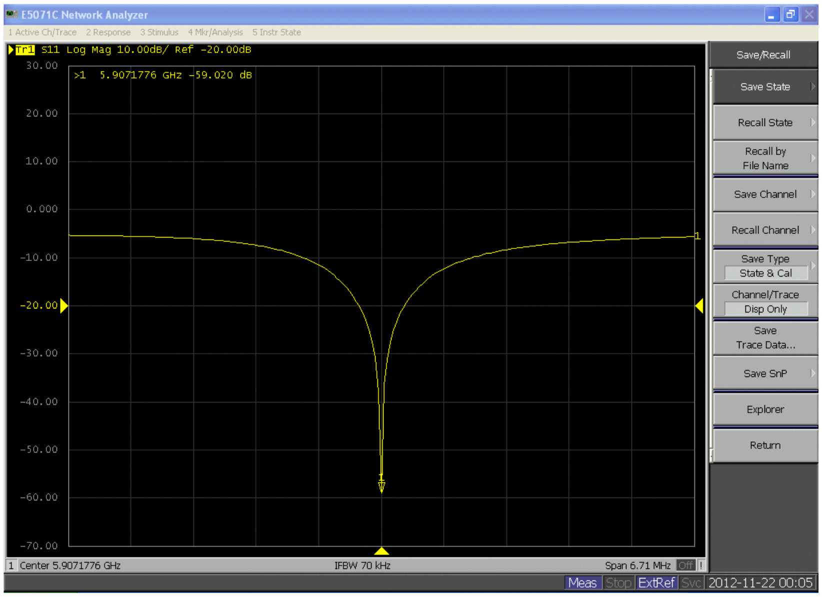

Figure 3.9. Resonance frequency (maximum attenuation in signal) for a 6 GHz Nb-cavity at room temperature.
An exact value of frequency can be read on top-left side of screen.

Once the cavity is locked it is desirable to work as close as possible to the critical coupling, where the reflected power is zero. By adjusting the location of the input antenna and the loop phase, one is able to minimize the reflected power and maximize the cavity gradient. Desired values of reflected power are under 2%.

When the critical coupling is set, the decay time measurement is performed. The relevant cavity parameters are calculated and the important data are saved automatically.

After that the laboratory is evacuated and all measurements are executed via remote computer control. This is done moreover to avoid ionizing radiation hazards.

The following steps should be repeated to record the *Q-E* curve using the INFN developed software:

1. turn on the amplifier;
2. turn on RF on the control panel;
3. search and lock the cavity, according to the above given procedure;
4. perform a Q_0 (decay) measurement, and save the set up file (*.set);
5. click on the "Q(E)" button: the curve begins to be displayed on the control panel;
6. gradually increase the power, always saving the recorded points when they are believed to be stable.

In order to reach 1.8 °K, the helium pressure must be reduced to about 15 mbar. Indeed at this pressure, a corresponding temperature of ~ 1.8°K, liquid helium is below the superfluid lambda point of about 2.17°K. Superfluid helium has better thermal conductivity which eases the process of keeping a cavity cold.

While the measurement procedure seen above is very similar between 6 GHz elliptical type and 101 MHz QWR, a very detailed explanation of QWR preparation procedure can be found at [7].

3.5 *Software*

The control program, developed in Visual Basic 3, allows to:

- calibrate the RF lines,

- find the resonant frequency,
- set the loop phase,
- lock the generator to the resonator frequency,
- adjust suitable coupling conditions and the forward power level,
- measure the levels of pick-up, forward and reflected power signals,
- measure the decay time,
- compute the Q_0 and plot it as a function of the accelerating field E, allowing both a fast data analysis and recording .

All these procedures are started from the program panel (fig. 3.10): the main control panel is designed to give complete manual control of the measurement, indicating all the crucial system parameters in real time. The automatic procedures are activated by the buttons and after completing the process, the system returns to the manual mode.

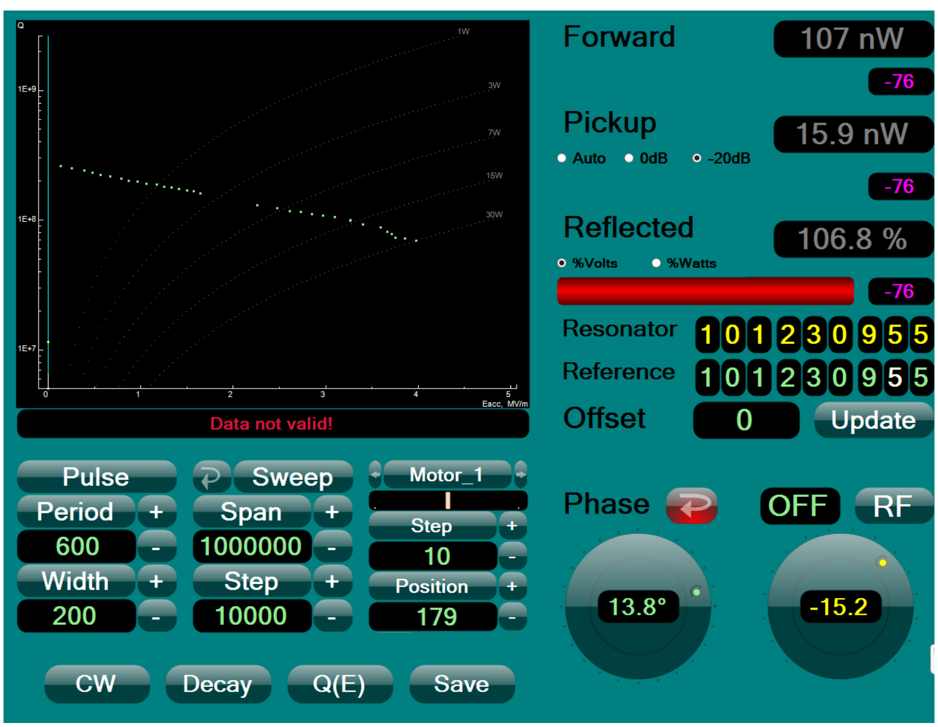

Figure 3.10. *Screenshot of the RF control program developed at LNL.*

The control panel is composed of numeric controls and indicators, indicator bars, several scroll bars and a custom menu. Starting from the right part of the screen (figure 3.10):

- The power indicator ("*Forward*") gives the power delivered to the cavity. The operator should be always aware of this value during high power operation as it is possible to exceed the power ratings of various components, leading to permanent damages.
- The "*Pickup*" indicator shows the power level transmitted by the resonator. It gives hints of the loop effectiveness. It is possible to change the sensitivity of the pickup power head between "*High*" and "*Low*" or leave it in an automatic mode.
- The "*Reflected*" power indicator: this is the ratio, in percent, of the reflected power divided by the forward power. It can be expressed in "Power" or "Voltage" percentage.
- It is important to minimize this signal in order to improve the measure accuracy.

Each power indicator displays a value, expressed in Watts, referenced to the cavity ports.
The software applies all the calibrations factors before displaying the data. The bar graph indicator below each box changes length and color when the displayed value enters three different ranges. In the boxes below the power indicators, the violet value expressed in dB, indicates the power read directly from the respective power head.

- The "*Resonator*" box, placed under the *Reflected* indicator, displays the actual loop frequency.
- Just below there is the generator frequency setting ("*Reference*"). It is also the sweep center frequency of the graph placed on the left and it can be adjusted by the operator.
- The "*Offset*" appears as number and position of the cursor in the indicator bar. It is the phase error signal coming out from the dc amplifier.
- The "*Phase*" provides a user control of the loop phase setting.
- The "*Power*" slider is in logarithmic scale and it allows one to increase or decrease the power from the amplifier.
- The "*Follow*" box sets the generator frequency to the resonant frequency of the cavity.
- The "*Lock*" box closes the loop.

- On the graph box placed on the left the frequency is spanned by the sweep. The frequency range could be selected with the scroll bar of the "*Span*" buttons, and, accordingly, the step width (of course the sweep is a discrete sequence in the frequency domain, with a given step).
- The "*Scan*" modality shows the pickup signal intensity versus frequency on the graph box.
- The "*Pulse*" modality switch on the pulse power for the cavity conditioning. "*Period*" and "*With*" of the pulse can be changed.
- The "*Q(E)*" button change the graph box to display the Q versus E curve. Each point of the curve can be registered in a file with the "*Save*" button.
- The "*Decay*" button starts the decay time calculations.
- The “*CW”* button go back to the normal procedure and it is used to go out from the "*Decay*" and "*Q(E)*" modality, or from pulse modality.

Another simpler but important software have been developed for the coupler motion. A stepping motor lift up and bring down a tube connected to the lamellar bellow of the antenna. The stepping motor could be controlled acting on the "*Speed*", the number of "*Steps*" and the movement direction (up or down).

This software allows to complete an RF measurement remotely, controlling all instruments and measurement parameters. The software is programmed to display several warnings in case of problems occurring during the test.

Some auxiliary systems for data acquisition, remote control

The setting of experimental apparatus requires keeping a large number of parameters under control. A large variety of test devices, which have to be quickly set and configured according to the different situations have to be used. Since for safety reasons the operators control the system remotely, a software tool was developed to make the acquisition and visualization process easier. It allows to configure the system: to get readings from all the connected devices, to register and visualize the data on the main computer and share them in the local network. The software is compatible with most Windows versions and is written in a way to minimize the load on the local network. The acquisition program, called GUARD, running on a computer located nearby the acquiring instruments makes the data available through the local network and the user can have real time visualization of data using the program, called CHARTS (fig. 3.11)[20].

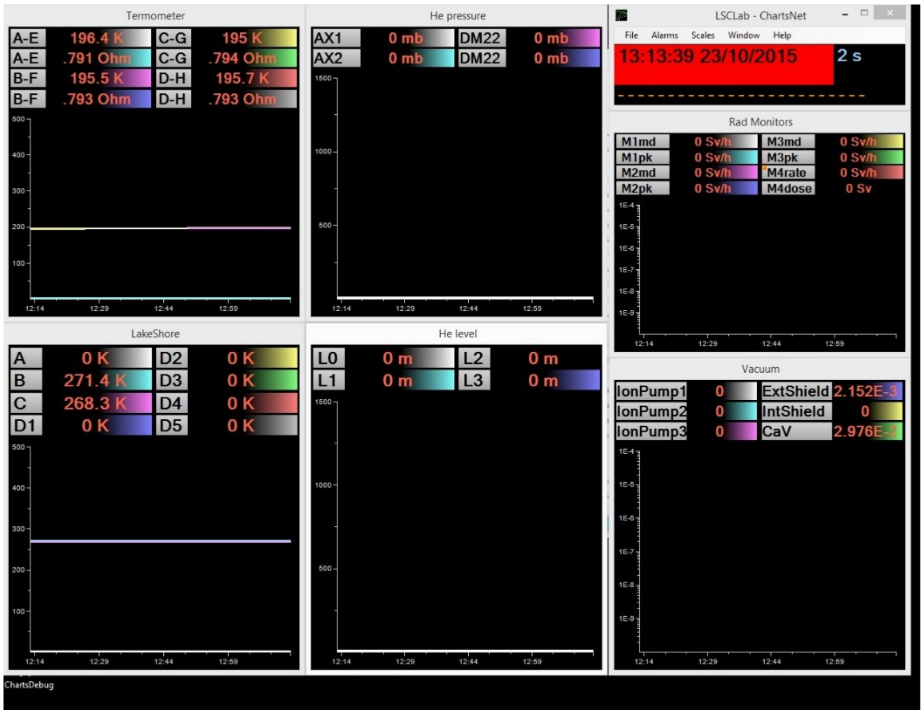

Figure 3.11. *Screenshot of the monitoring real time visualization of data software CHARTS, developed in Visual Basic 2005 in order to draw all monitored data collected by the software GUARD.*

GUARD presently supports data acquisition from the most typical instruments used in the lab for thermometry, cryogenics, vacuum, pressure, radiation, frequency, RF, AC, DC measurements and data available from other computers through the local network.

Figure 3.11 shows, from the left side of the screen, indicators for the cavity and stand temperatures, pressure in the different chambers of the cryostat, helium level in the cryostat, cavity vacuum pressure and radiation monitor signals.

3.6 *Radiation Safety System*

During the RF test, a cavity may become a source of ionizing radiations. Electrons are emitted from the walls of the cavity and then accelerated by the presence of the high intensity electric field.

This electron current generally hits the wall of the cavity and X-rays are produced by Bremsstrahlung effect. The electrons heat the material and, at high enough levels, may cause a local hot spot which leads to a quench of the superconducting state. The performance of the resonator drops exponentially and the test stops. The occurrences for this event have been thoroughly studied over the last 40 years and it turned out that they are usually associated with the cleanliness of the surface and many procedures have successfully been developed to eliminate this problem.

However, since the potential for radiation exists, a safety system is mandatory to monitor the emitted radiation dose. Each cryostat stays in a concrete pit with a wall thickness of at least 15 cm and it is laterally shielded with 1.5 cm lead. The cryostat top plate is made of a 2.5 cm stainless steel plate and 4 mm Aluminum plate.

Three detectors are interlocked to the main RF Power Amplifier and continuously monitor the radiation emitted during the measurement. Values above the security threshold automatically turn off the amplifiers. Once there is no power to the cavity, the radiation emission stops and, since there is no process of activation, the access to lab is safe again. Before starting any high power tests the operator has to check the presence of any possible worker and advise them to leave the room. In addition, an acoustic alarm and flashing signals warn individuals outside the lab that a production of radiation may occur.

Several check-point buttons are present inside the laboratories and the operator has to press in the right order as part of the search procedure which is used to ensure that nobody is present in any of the areas where there is a potential for ionizing radiation above regulatory thresholds.

The amplifier can be switched on only when all the check-points are done and the door to the external corridor is closed. For security reasons, there are also thirty seconds before the activation. This allows anyone still inside the laboratory to be able to press the emergency button which inhibits operation. All the doors are interlocked to the main power by making use of several micro-switches. Disturbing these interlocks will also crash the system to a safe state.

Chapter 4

Experimental results

4.1 *Test cavities*

The research work reported in this dissertation mainly focuses on a set of three 6 GHz elliptical type cavities fabricated using spinning technique, as seen in section 1.6, to create seamless structure (fig. 4.1). Every single cavity is equipped with two thermometers providing a feedback on the temperature. Several external surface treatments have been applied and a comparison of "before/after" performance has been studied.

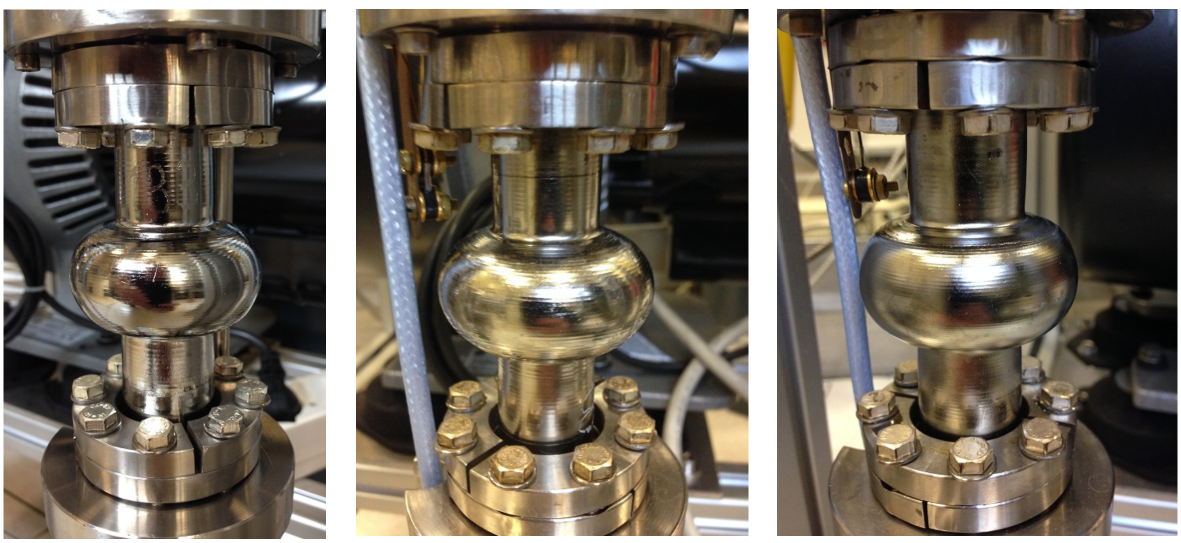

Figure 4.1. a) Cavity n. 133 b) Cavity n. 188 c) Cavity n. 134

The first investigation (n.133) was aimed to study the influence on cavity performance of external surface conditions, limited to the bulk situation without any thin film coating. Specifically, after a first RF measure on a polished surface, an opacity test has been performed by a mechanical scratch of the external wall and then a new RF measure took place. Eventually, the cavity has been baked at 80°C for 3 days for a last RF characterization.

In the second case (n.188 and n.134) the attention was moved to investigate a possible influence of the interface between bulk niobium and the copper thin film. In real situation the cavities used in particle accelerators are made of copper internally coated by a thin niobium film, but a more practical choice was pursued being aware of that. A first RF test has been then performed followed by a sputtering process to coat the external surface and see how the performance would have been affected.

As a secondary activity, an RF test has been carried out on the 101 MHz Nb-Cu QWR cavity in order to compare the performance with previous measurements carried out last year. For a detailed explanation of the surface treatments that the QWR has undergone see [7].

4.2 *RF tests results*

4.2.1 *6 GHz elliptical type cavity n. 133 - Opacity test*

Before moving to study the Cu-Nb interface, a preliminary test was conducted, focusing on the bulk external surface without any thin film coating.

Figure 4.2. *Bulk Nb cavity n.133.*

After the assembling of cavity n.133 inside the clean room, it was mounted on the vertical stand (fig. 4.3) and connected to the pumping system for a preliminary vacuum usually reached after an all-night-long process. At 10^{-6}-10^{-7} mbar the ion getter pump was turned on to further decrease the vacuum. The stand was disconnected from the pumping system and inserted into the cryostat. At this point, the transfer of the cryogenic liquids started with liquid nitrogen first, followed by liquid helium. The vacuum eventually reached 10^{-8}-10^{-9} mbar.

Literature on dependence of the Q factor on the cooling dynamics is abundant [21][22][23][24]; in this case no thermal cycling was induced, only a slow cool down process was followed.

Once the cavity was completely immersed in the helium bath and both the thermometers measured a temperature of 4.2°K, indicating a thermal equilibrium, a cables calibration was performed before the lab was evacuated. A first Q vs E curve was measured by slowly increasing RF signal power driven to the cavity. At 4.2°k, due to unknown issues, it was very hard to raise the power and reach an E_{acc} much higher than 2 MV/m.

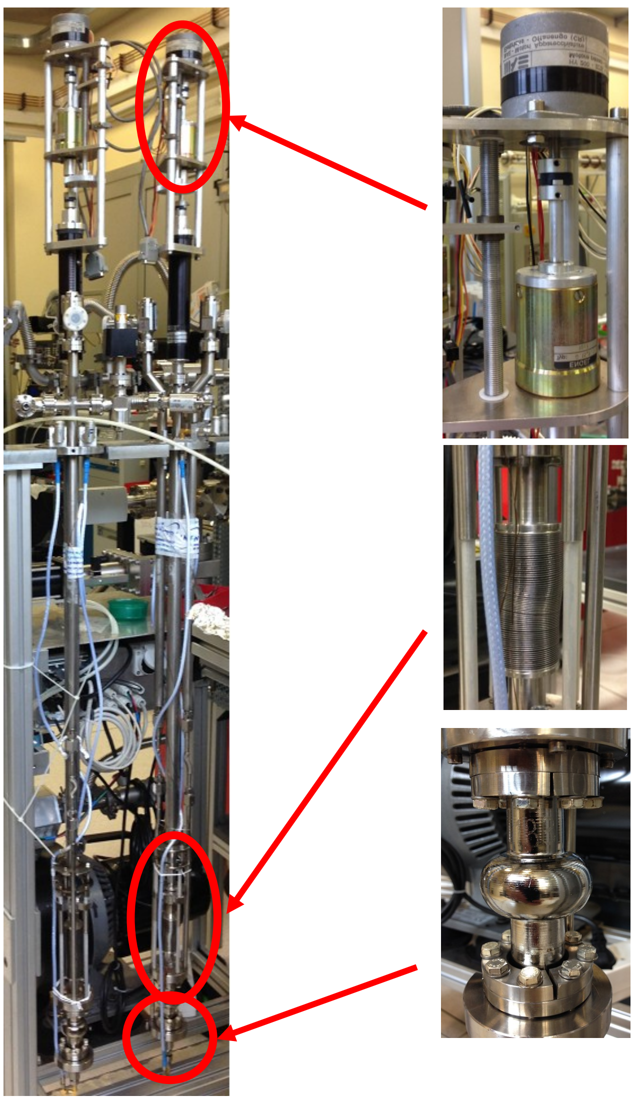

Figure 4.3. *Bulk Nb cavity n.133 on its stand.*

Then the pressure above the helium bath was slowly lowered to cool down the system at 1.8°K. After it was stabilized, a new set of data was taken. This time a higher accelerating field was achieved. In figure 4.4 a plotting of the data acquired shows the quality factor trend in both cases.

External surface treatment: Mechanical scratch

The next step was to mechanically scratch the external cavity walls, thus having a matt surface in contact with the liquid helium. The aim was to understand whether a matt surface could aid the thermal transfer from the cavity to the bath, compared to a polished surface, by preventing phonons reflection at the interface. This should lead to an improvement of the quality factor.

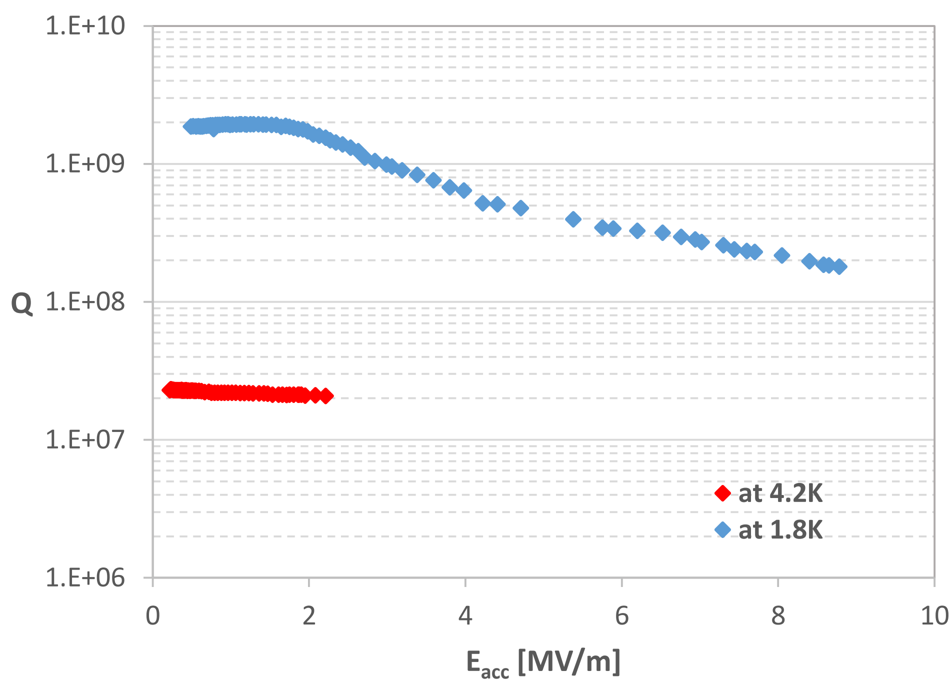

Figure 4.4. *Bulk Nb cavity n.133: RF test at 4.2 and 1.8 °K.*

The mechanical operation was performed keeping the cavity on its insert, as shown in figure 4.5, preferring to avoid a vacuum breaking in order to maintain the previous internal conditions as far as possible.

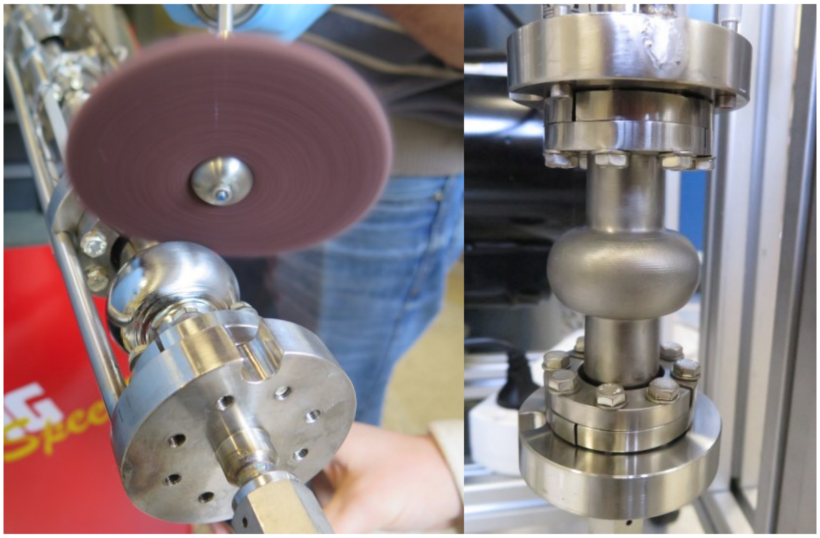

Figure 4.5. *Mechanical treatment of cavity n.133.*

Comparing the newly obtained quality factor with the previous one, a very sharp deterioration was evident (fig. 4.6). Not of little importance, the strong mechanical excitation must be considered. This could have supposedly promoted some dust detaching from the internal walls, that could have affected the performance, or the mechanical treatment could have simply deteriorated the cavity.

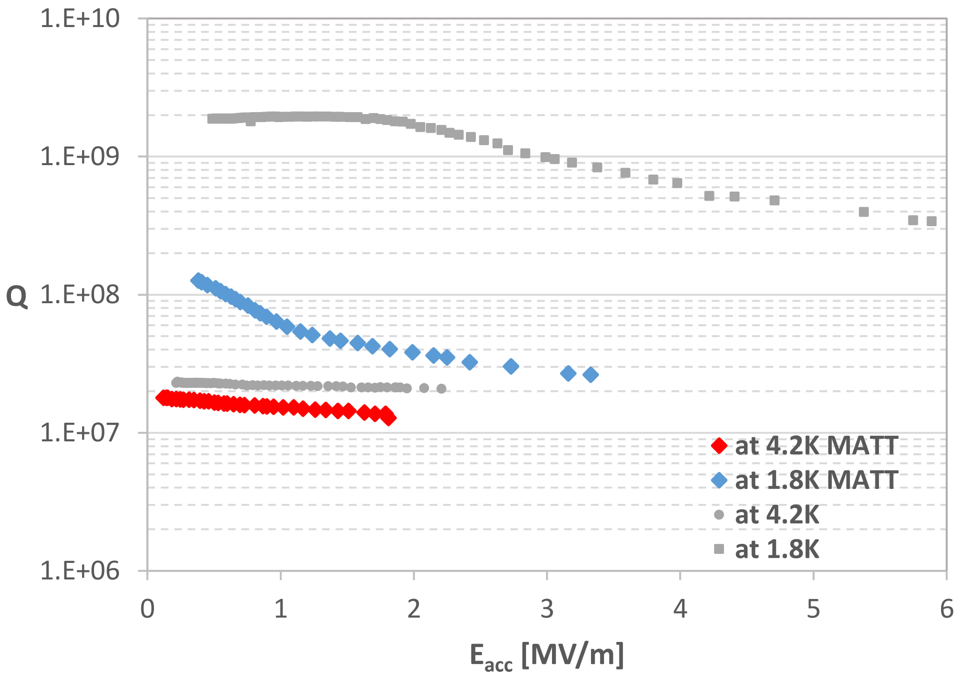

Figure 4.6. *Bulk Nb matt cavity n.133: RF test at 4.2 and 1.8 °K.*
In grey are reported the curves of polished cavity.

Baking process

A further step was to let the cavity undergo a gentle thermal treatment at 80°C for 3 days, while in vacuum, to force outgassing and test it with RF once again. A higher baking temperature was not advisable, due to the risk of liquefaction of the vacuum grease used to seal the bottom and top flanges (see section 3.4). For this purpose, a resistor heating band had previously been wrapped around the cavity as can be seen in figure 4.7.

One more time, the obtained curves from the RF test were compared with the last measurements (fig. 4.8). A clear improvement of performance was registered from the "matt" situation, indeed the curve shapes the trend of the very first "polished" situation but in a narrower range of accelerating field. As from the graph the *Q* did not rise above the 4.2°K of the "polished" case and did not approach its 1.8°K line.

Figure 4.7. *Baking of the bulk Nb matt cavity n.133.*

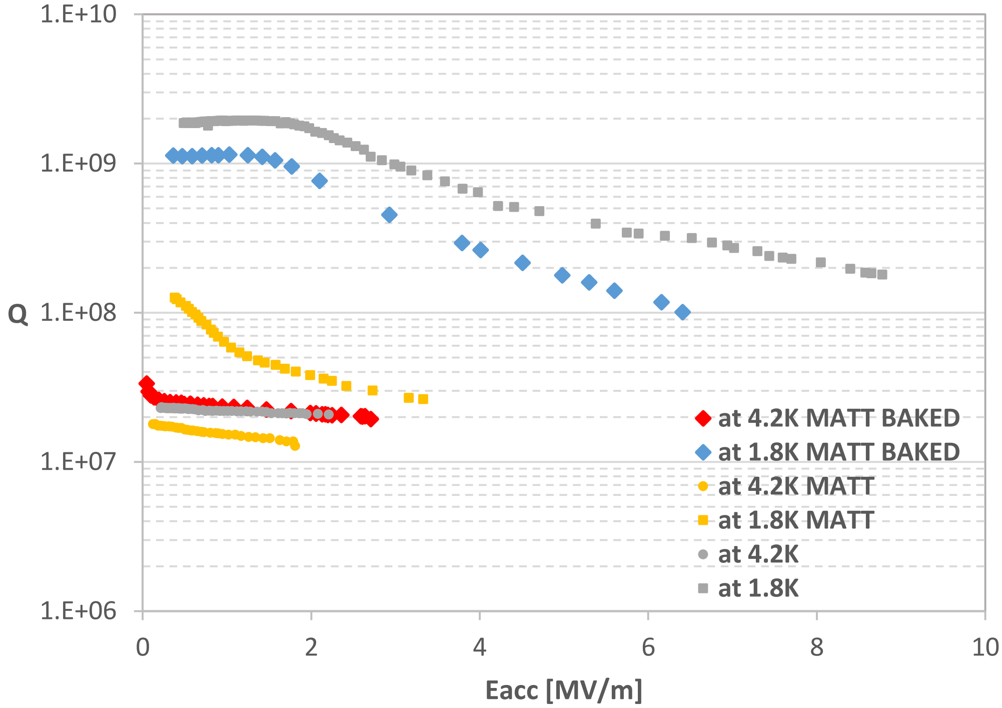

Figure 4.8. *Bulk Nb matt and baked cavity n.133: RF test at 4.2 and 1.8 °K.*
In grey the curves of polished cavity are reported.
In black the curves of matt cavity are reported.

4.2.2 *6 GHz TESLA type cavity n. 188 – Cu-Nb interface study*

With cavity n.188 the attention has been moved on the Cu-Nb interface in order to estimate the possible influence of a thermal boundary resistance between niobium and copper surfaces. Since this influence could be not negligible, the overall resistance may increase and affect the cavity performance. For the purpose, another bulk niobium cavity was chosen and tested before being externally coated by a copper thin film. This time, the cooling process (in both bulk and Cu-Nb cases) was faster but a thermal cycle was induced, in which the cavity is briefly warmed above the transition temperature of 9.2 K and cooled down again.

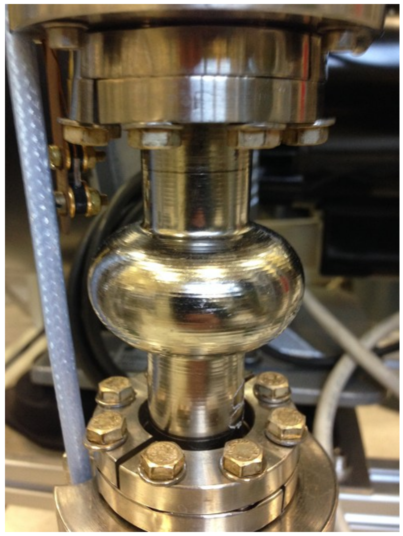

Figure 4.9. *Bulk Nb cavity n.188.*

In a real situation the cavities used in particle accelerators are made of copper internally coated by a thin niobium film. For the effect meant to be investigated, the external treatment was the preferable choice both for an easiest procedure of thin film deposition and for allowing a test on the bulk situation first. An RF test with the bulk cavity was then performed and the data were plotted in figure 4.10.

While at 4.2°K the Q curve seemed to shape the one registered for the cavity 133, at 1.8°K the resonator started quenching much sooner. That was probably due to the different way in which the treatments involved, from the fabrication to the assembling, affected the cavity performance. For a brief introduction to the surface treatment techniques commonly applied see [25].

Once the measure was finished, the cavity stand was pulled out from the cryostat and the preparation for the following sputtering process started.

External surface treatment: Cu thin film coating

Magnetron sputtering technique has been applied, which was the best choice for the purpose. The studied configuration planned to use a planar magnetron equipped with a copper target (fig. 4.11) and placed horizontally on the side walls of the chamber (fig. 4.12). In this way the rotation of cavity

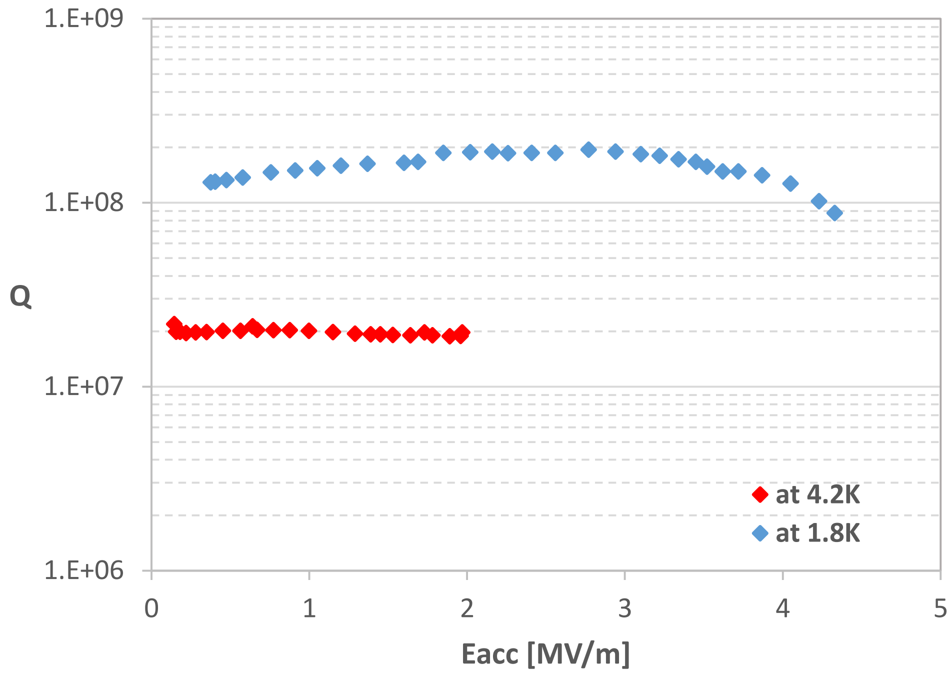

Figure 4.10. *Bulk Nb cavity n.188: RF test at 4.2 and 1.8 °K.*

insert inside the chamber, made possible by means of a step motor flanged at the top and supporting the whole structure, allowed the external cavity surface to face the plasma produced in front of the target and be uniformly coated. Figures 4.13 and 4.14 respectively show the insert attached to the step motor and the plasma acting inside the chamber. Even in this case the cavity remained in its insert to preserve the experimental conditions. An aluminum foil prevented the insert from being sputtered (fig. 4.13).

At first, a cavity test was used to make sure the thin film deposited did not peel off from the surface coated. This was important since a bad adhesion between the copper film and the niobium substrate is one of the hypothesized responsible for a poor thermal transport.

A stress test was carried out, in which a strong thermal shock was imposed by immersing twice the test cavity into liquid nitrogen and immediately warming it up with hot air at 200°C after each submersion (fig. 4.15). No visible sign of peeling off were observed.

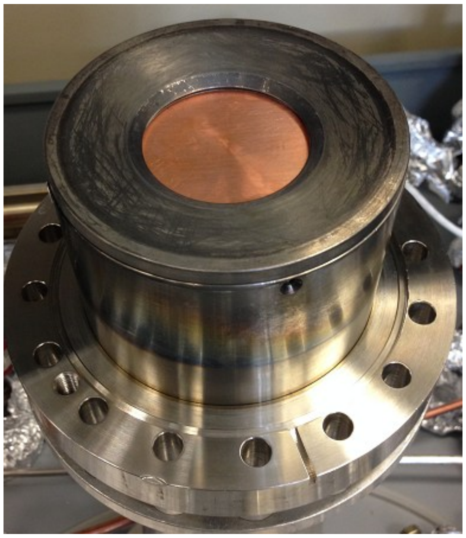

Figure 4.11. *Planar magnetron.*

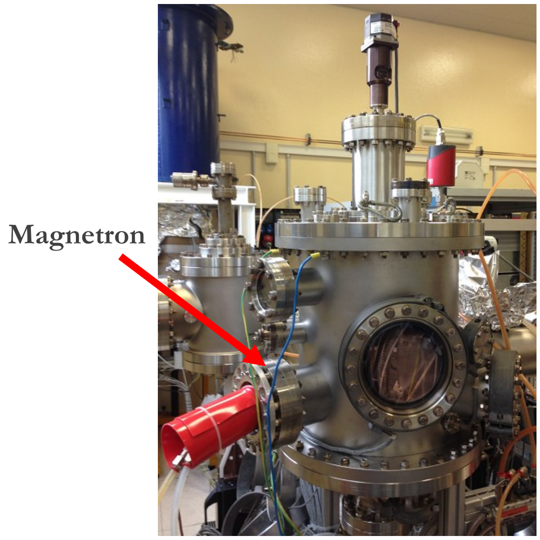

Figure 4.12. *Sputtering chamber.*

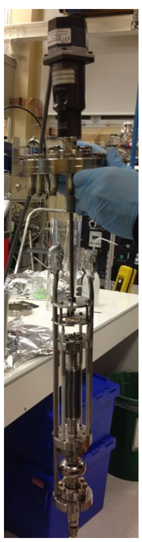

Figure 4.13. *Cavity support.*

Figure 4.14. *Sputtering process.*

Figure 4.15. *Stress test on test cavity.*

At this point the cavity n.188 was ready to be sputtered. The process pressure was set at 8/9x10^{-3} mbar and lasted 30 mins divided in two runs of 15 mins each with a stop in between to let the system cool. A stable current of 0.5A between the target (cathode) and the grounded cavity maintained the plasma in operation. The parameters were chosen to make a thin film of approximately 2 μm of thickness. Figure 4.16 shows the cavity once out of the chamber at the end of the sputtering process.

The test on Cu-Nb cavity was performed either at 4.2 and 1.8 °K. At 1.8 °K it was only possible to collect data up to an E_{acc} of 1.6 MV/m, because the reflected power could not be minimized (fig. 4.17).

Figure 4.16. *Cu-Nb cavity n.188.*

No significant deviation of the curve from the bulk state was observed. A slightly higher Q values were observed at 1.8°k and at low fields but these are likely to be a pointless reference because of the above mentioned problems.

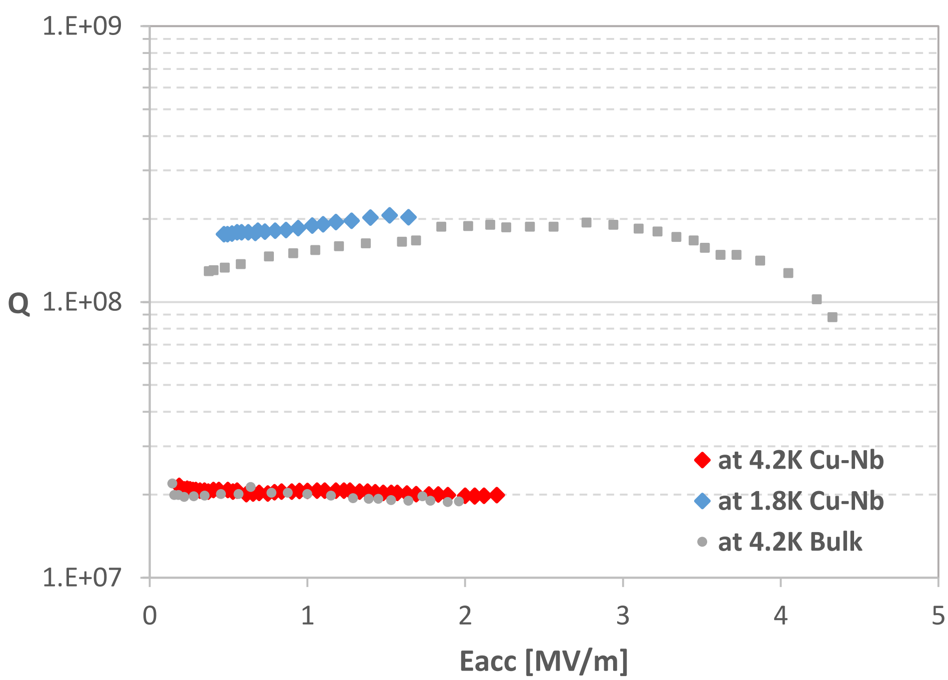

Figure 4.17. *Cu-Nb vs Bulk cavity (in grey) n.188: RF test at 4.2 and 1.8 °K.*

4.2.3 *6 GHz TESLA type cavity n. 134 – Cu-Nb interface study*

Next cavity was the n.134. The first measure, in bulk state, took place simultaneously with bulk cavity n.188 since the cryostat can house up to three 6 GHz elliptical cavities as seen in section 3.3. Once again a fast cooling process (in both bulk and Cu-Nb cases) was followed but a thermal cycle around T_c as seen for the cavity 188.

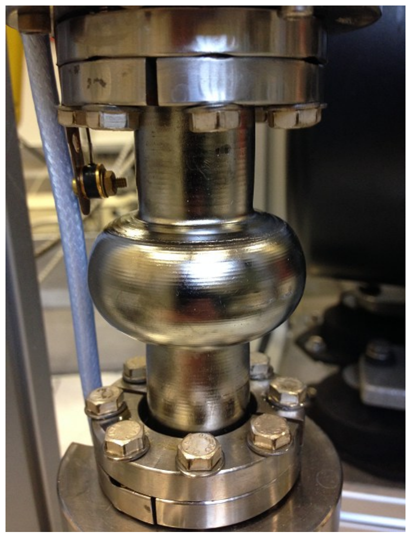

Figure 4.18. *Bulk Nb cavity n.134.*

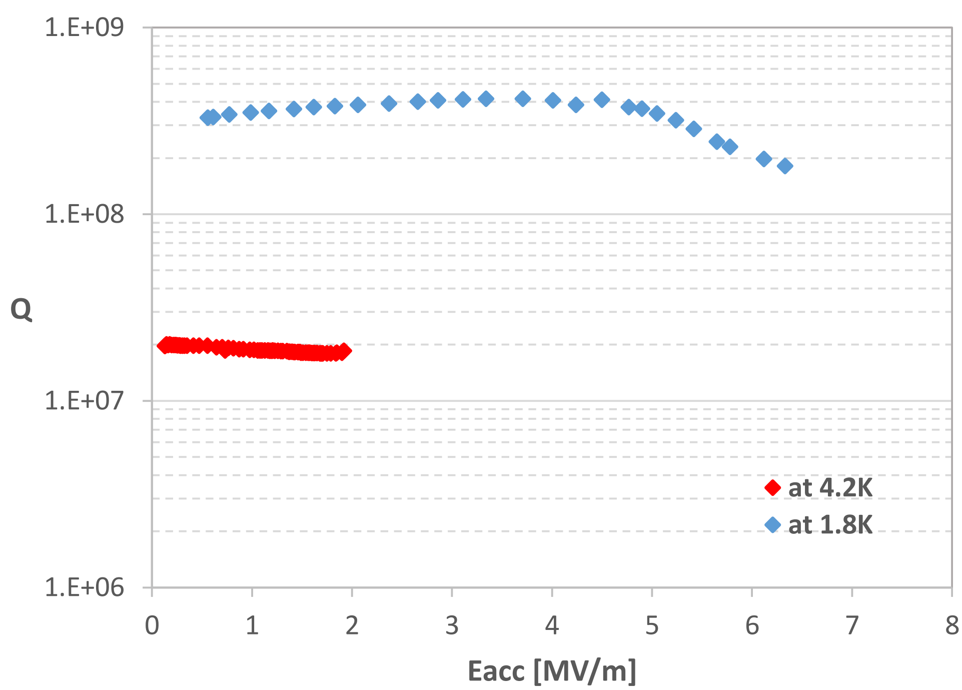

Figure 4.19. *Bulk Nb cavity n.134: RF test at 4.2 and 1.8 °K.*

Figure 4.19 shows the trend of the experimental Q values registered. As can be easily seen from the graph the 4.2°K curve perfectly match the 188 bulk case. At 1.8°K the quality factor, although of the same magnitude order, is slightly higher. Overall the comparison exhibits a very similar behavior.

External surface treatment: Cu thin film coating

Moving to the Cu-Nb inspection, even for the cavity 134 the sputtering process parameters of the previous 188 were maintained and figure 4.20 shows the result.

Figure 4.20. *Cu-Nb cavity n.134.*

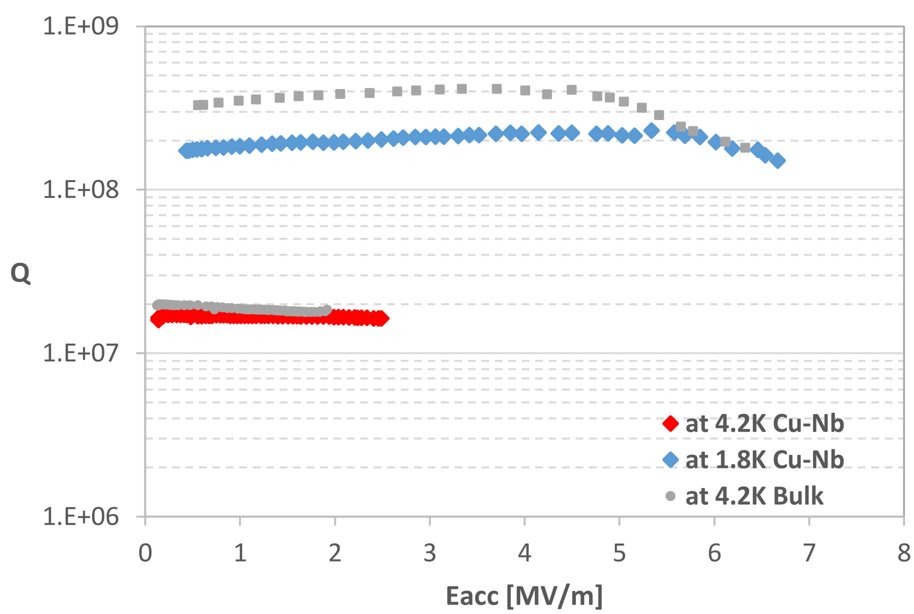

Figure 4.21. *Cu-Nb vs Bulk cavity (in grey) n.134: RF test at 4.2 and 1.8 °K.*

Another graph of comparison was then charted in figure 4.21. A brief analysis clearly reveals a light *Q* deterioration at 4.2°K, even though the field raised above 2 MV/m. An evidence of stronger deterioration appeared at 1.8°K, but this time the coated cavity started quenching later then the bulk one.

4.2.4 *101 MHz QWR cavity*

In the framework of a LNL-CERN collaboration aiming to study and improve the present deposition techniques on copper QWRs dedicated to HIE-ISOLDE linac at CERN (fig. 4.22), a new magnetron configuration source was tested at INFN-LNL and several RF tests are ongoing. In particular, the influence on superconducting properties of two principal parameters of the sputtering process has been studied: the power and the substrate temperature [7]. The speed of magnetron rotation was also taken into consideration.

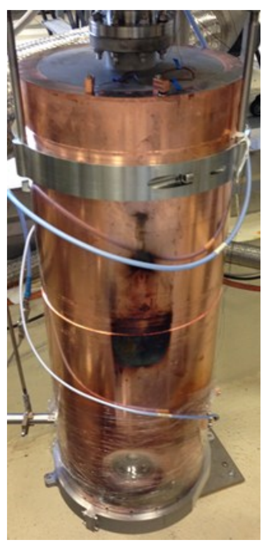

Figure 4.22. *Nb-Cu QWR cavity.*

What follows is a brief summary, taken from the above mentioned literature, of the previous RF tests and respective deposition processes performed before the present work started. The curves of the quality factor obtained in each measure will be then reported and compared with the last test carried out so far.

Prior to deposition, the cavity was treated at CERN and sent to LNL where it was placed inside the vacuum chamber to reach the pressure necessary to perform the deposition.

With a base vacuum of around 10^{-6} mbar an outgassing was performed for 72 hours to improve the vacuum. For this purpose the vacuum chamber was baked at 170 °C while the copper cavity was baked at 400°C, reaching a final vacuum of 10^{-7} mbar. Figure 4.23 shows the parameters used in the first run of deposition.

Deposition	Sputtering Pressure (mbar)	Base vacuum (mbar)	Power (kW)	Current (A)	Voltage (V)	Time (min)	Heating °C
1	1e -2	1e-7	30	75	408	40	450

Figure 4.23. *Parameters used to perform the first sputtering over the copper QWR.[7]*

At the end of the baking procedure the system was left cooling for several days before removing it from the vacuum chamber.

Figure 4.24. *QWR cavity before (left) and after (right) the Nb deposition. [7]*

After the sputtering process the cavity was taken to the clean room where the tuning plate was mounted on it. The electric contact between the cavity and the plate is ensured by mechanical clamping with 72 screws tightened at 5 Nm each [26].

Figure 4.25 shows the cavity during the mounting of the tuning plate.

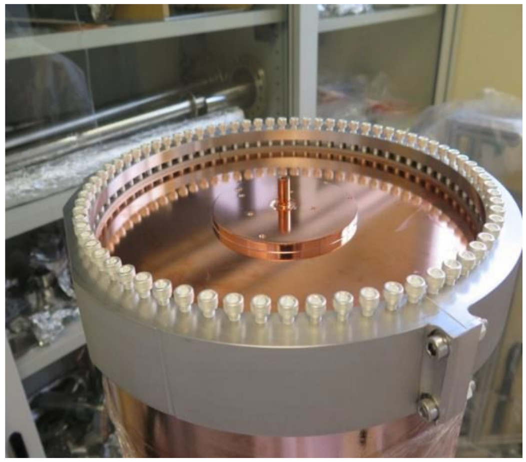

Figure 4.25. *Nb-Cu tuning plate deposited at CERN. [7]*

After assembling the antennas (pick-up, coupler), thermometers and coupler motion, the QWR was fixed on the cryostat stand (fig. 4.26) and placed inside the bunker to start the pumping. The cryostat was pumped to reach a vacuum around 10^{-6} mbar and then the cavity was baked at 100°C for 8 hours with an IR lamp. This was placed inside the inner conductor (the one later filled up with liquid helium).

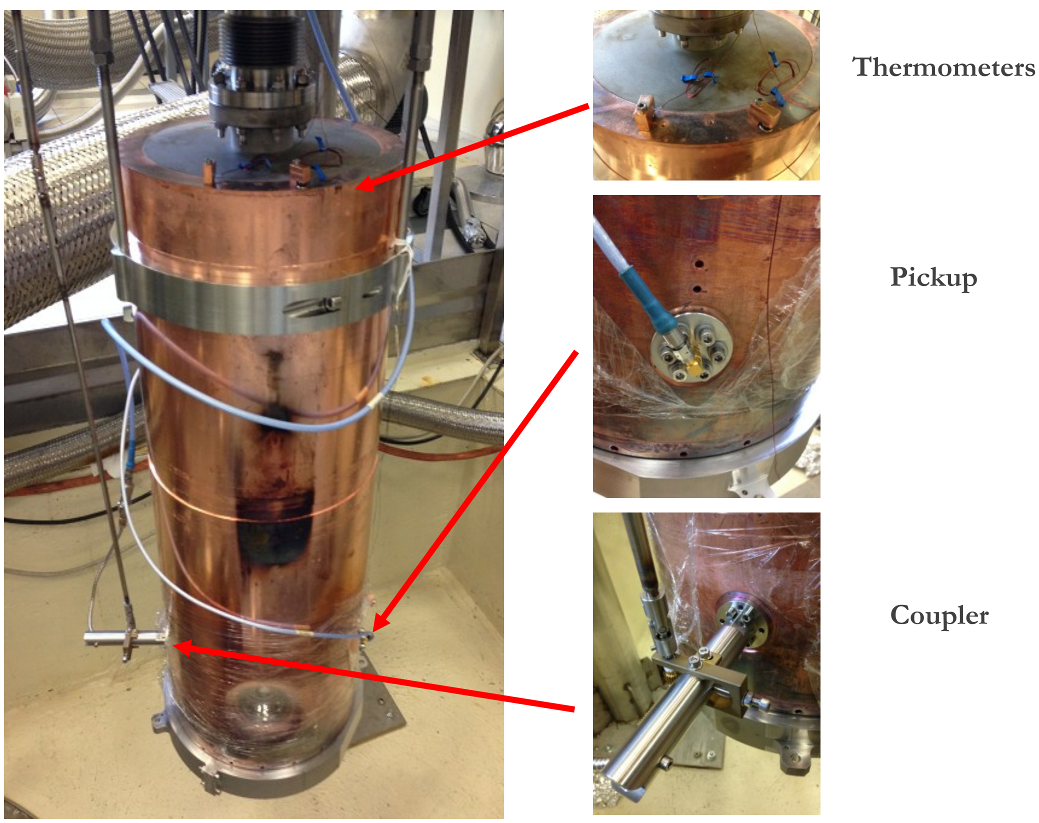

Figure 4.26. *Nb-Cu QWR cavity assembled.*

Once the baking process ended, the cooling of the system started injecting liquid nitrogen first, followed by liquid helium up to reach 4.2°K.

A major performance limitation is the multipacting, which is a resonant process in which an electronic avalanche builds up within a small region of the cavity surface giving rise to a local hot spot. To avoid this drawback, a process of both warm and cold conditioning was performed: the first during the cooling, but before reaching $T_{c,}$ while the second at 4.2°K. It consists, essentially, in a power sweeping in which the cavity was fed with a power up to 5 W for several hours, while out of resonance keeping the reflected power above 50%. The conditioning aim is always to "touch" the surface area with RF, "burn" particulates and induce controlled gas layers desorption (they enhance the secondary electron emission coefficient and cause "local desorption outbursts" which could facilitate arcing events) [27].

The cavity was then tested and the Q curve plotted in figure 4.28 (blue line) showing a strong decay at very low fields. The reason was hypothesized to be the thin niobium layer which did not replicate the bulk situation. Starting from this, another sputtering run was performed over the first layer for the same time to double the thin film thickness. Although the conditions were maintained almost the same (fig. 4.27), an increased temperature of the substrate were set to give more uniformity to the deposition. The second RF test returned a Q trend (green line) with a stronger and faster decay from the beginning.

Deposition	**Sputtering Pressure (mbar)**	**Base vacuum (mbar)**	**Power (kW)**	**Current (A)**	**Voltage (V)**	**Time (min)**	**Heating °C**
2	1e -2	8.2e-8	30	75	410	40	550

Figure 4.27. *Parameters used to perform the second sputtering over the Nb-Cu QWR.[7]*

One plausible explanation could be correlated to impurities from the first coating. For this reason, another RF test, performed under this work, was carried out after a complete removal of the thin film deposited followed by a new deposition (parameters in fig. 4.28). This time the focus was on getting an even more uniform deposition, and on improving the outgassing to reduce the influence of impurities.

Deposition	Sputtering Pressure (mbar)	Base vacuum (mbar)	Power (kW)	Current (A)	Voltage (V)	Time (min)	Heating °C
3	1e -2	8.2e-8	30	75	380	30	550

Figure 4.28. *Parameters used to perform the third sputtering over the Nb-Cu QWR.*

After all the cleaning and assembling procedures the QWR was ready for the new RF test and this time the power supplied during the conditioning was raised up to 25 W. Red line in the graph of figure 4.29 reproduces the trend registered.

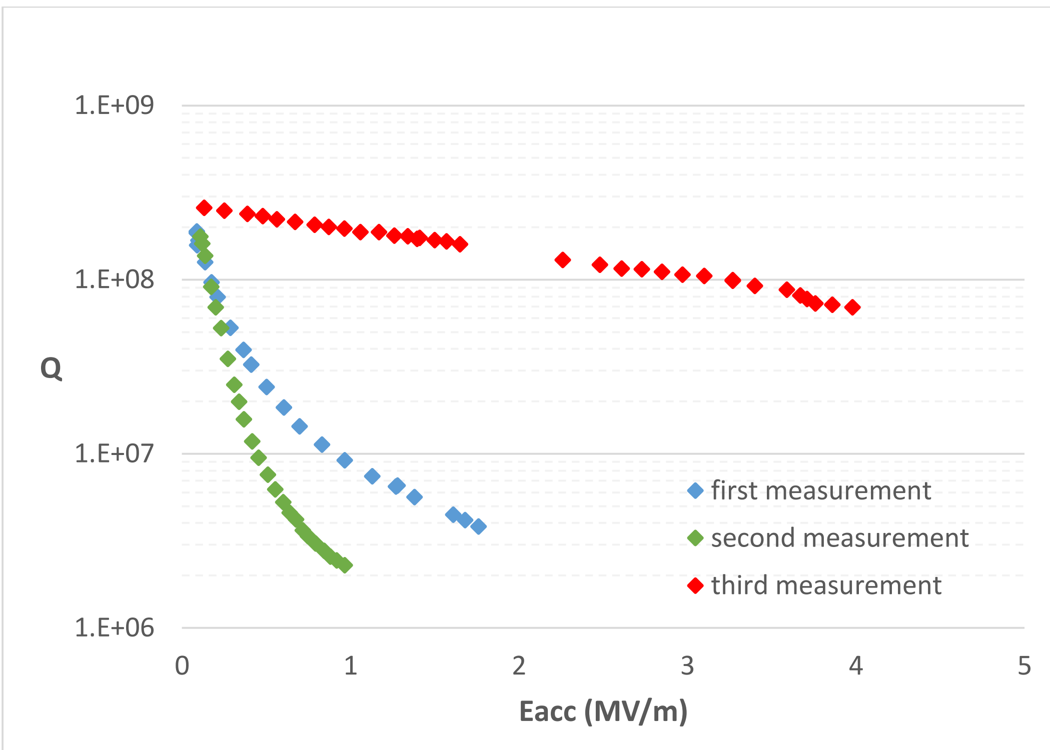

Figure 4.29. *Nb-Cu QWR cavity measurements: RF test at 4.2°K.*

An evident improvement of performance were observed, with a more linear behavior of the quality factor at increasing accelerating field, thus approaching CERN specifications of $Q \approx 5x10^8$ and $E_{acc} \approx 6MV/m$.

Conclusions

Starting from mechanical treatments and moving on through sputtering deposition, the aim of this work was an attempt to better understand of how external surface, thin film layers and interface between thin films and substrates could affect the performance of superconducting cavities. This is not a trivial issue at all, from the comprehension of which the future of particle accelerators will strongly depend on for pushing forward the actual technical limits.

Ideally, the cavity quality factor should remain constant at increasing accelerating fields up to the point of a critical magnetic quench field, but actually the resonator is quenching before, due to imperfections and impurities of the material.

As a premise, the experimental evidences, the below considerations are based on, are certainly not enough to draw definitive conclusions. More tests involving a wider range of cavities should be conducted. The following could be considered as observations rather than strong proofs.

The first study, conducted on a bulk niobium 6 GHz elliptical cavity (n. 133) was aimed to point out any influence of the external surface opacity on the resonator performance. The idea that a matt surface could promote phonons transmission helping the thermal transfer to the helium bath, cannot be stated since the mechanical treatment involved could have deteriorated the cavity.

The second research work focused on the interface between copper and niobium, specifically between bulk niobium and copper thin film, trying to determine whether a thermal boundary resistance could significantly affect the overall cavity resistance and consequently influence the accelerating performance.

The predicted behavior, a deterioration of the quality factor compared to the bulk situation due to the presence of the Cu-Nb interface, is in fact observed at 1.8°K in cavity n.134, while cavity n.188 showed the opposite trend. However, it must be remarked that the experimental configuration adopted in the test, a copper thin layer on a niobium substrate, is the contrary respect the actual situation. Considering the higher thermal conductivity of copper compared to niobium and the difference in thickness (2mm Nb and ≈ 2μm Cu), it can be supposed that the poor contribution in thermal transfer of niobium could drive the heat dissipation and predominate over the effect of the thermal boundary resistance. This cannot be stated with certainty since both cavities were characterized by a quite low quality factor, which must hopefully be above 10^9-10^{10}. It means that other factors, such as impurities, could have contributed.

The last test aimed to measure a QWR cavity and just compare the performance registered after a new surface treatment, i.e. a new deposition of niobium thin film, with the previous measurements performed earlier. Some sputtering parameters have been changed and the collected data shows an improved quality factor, meaning that the way this research is following, however long and hard, seems to be the right way.

In conclusion, niobium thin films have not yet achieved their potential ultimate performance and further improvements in the surface treatments of superconducting cavities are required.

The ultimate goal for ideal accelerating superconducting cavities is achieving very high quality factor values at higher accelerating fields. These two aspects are the guiding stars in particle accelerator technology.

Bibliography

[1] V. Palmieri, *Seamless cavities: the most creative topic in RF superconductivity*, Proceedings of the 8th workshop on RF superconductivity (1997), vol. 3, P.553

[2] H. Kamerlingh Onnes, *Communications from the Physical Laboratory at the University of Leiden by Prof. Dr. H. Kamerlingh Onnes*, 108, 1908

[3] W. Meissner and R.Ochsenfeld, *Ein neuer Effekt bei Eintritt der Supraleitfahigkeit*, Naturwiss., 21, 787, 1933

[4] H. Padamsee, J. Knoblock and T. Hays, *RF Superconductivity for Accelerators*, Wiley and Sons, New York, 1998

[5] J.M. Pierce et al., In Proceedings of the 9th Inter. Conf. on Low Temp. Physics, Vol.A. Plenum, New York, p.36 (1965)

[6] A.T. Wu, *Use of Niobium for Fabricating Superconducting Radio Frequency Cavities,* Thomas Jefferson National Accelerator Facility USA

[7] D.A. Franco Lespinasse, *An Innovative Cylindrical Magnetron Sputtering Source For The Deposition Of Hie-Isolde Superconducting Nb/Cu Qwrs,* Ph.D. thesis, University of Padova (2014)

[8] Lanza G., *Technical Protocols for Processing, Sputtering and RF Measuring of Niobium-Copper Cavities,* Master thesis, University of Padova (2008)

[9] I. Ben-Zvi, *The quarter wave resonator as a superconducting linac elements*, Nuclear Instruments and Methods, vol. 212, pp. 73-79, 1982

[10] W. Meissner and H. Franz, *Messungen mit Hilfe von flussigen Helium. VIII.Supraleitfahigkeit von Niobium*, Physikalisch-Technische Reichsanstalt, Mitteilung: 558-559, 1930

[11] A. Inoue et al., J. Phys., Colloque-8. 41, 758, 1980

[12] J. Jackson, *Classical Electrodynamics*, Wiley, New York, 2nd edition, 1975

[13] K. Halbach and R. Holsinger, *Particle Accelerators* 7 (1976) 213 – 222.

[14] K. Schulze, The metallurgical society of AIME, 1981, P.163

[15] Gladun et al, Journal of Low Temperature Physics, 27 (1977) P873

[16] Kapitza P L 1941 J. Phys. USSR 4 181

[17] Khalatnikov I M 1965 Introduction to the Theory of Superfluidity (New York: Benjamin)

[18] V. Palmieri and R. Vaglio, *Thermal contact resistance at the Nb/Cu interface as a limiting factor for sputtered thin film RF superconducting cavities,* Supercond. Sci. Technol. (2015)

[19] G. Lanza, *New Magnetron Configurations For Sputtering Niobium Thin Films Into Copper Tesla-Type Superconducting Cavities*, Ph.D. thesis, University of Padova (2008)

[20] S. Stark, *GUARD - modular software for complex system monitoring and data sharing*, LNL Annual Report.

[21] A. Romanello et al, *Dependence of the residual resistance of superconducting RF cavities on the cooling dynamics around T_c*, Journal of Applied Physics 115, 184903 (2014)

[22] J.-M. Vogt et al, *Impact of cool-down conditions at T_c on the superconducting RF cavity quality factor*, Phys. Rev. Special Topics – Accelerators and Beams 16, 102002 (2013)

[23] O. Kugeler et al, *Improving the intrinsic quality factor of SRF cavities by thermal cycling*, In Proceedings of SRF2011, (2011)

[24] D. Gonnella and M. Liepe, *Cool down and flux trapping studies on SRF cavities*, In Proceedings of LINAC2014, Geneva (2014)

[25] R.K. Thakur, *Purification technique of 6 GHz Tesla type superconducting Nb cavities: A new approach for improving RF performances,* Master thesis, University of Padova (2013)

[26] R. Behrisch, *Sputtering by Particle Bombardment III*, in Topics in applied physics, California, Springer-Verlag, 1991, pp. 3-28.

[27] J. Weisend, The Handbook Of Cryogenic Engineering, Philadelphia USA: Taylor and Francis, 1998 Pp 259.